Accepted Manuscript

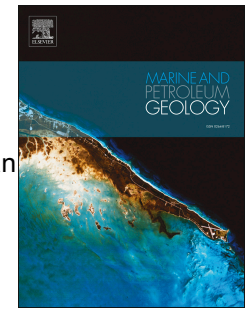

New insights on the Sorbas Basin (SE Spain): the onshore reference of the Messinian Salinity Crisis

Georges Clauzon, Jean-Pierre Suc, Damien Do Couto, Gwénaël Jouannic, Mihaela Carmen Melinte-Dobrinescu, Laurent Jolivet, Frédéric Quillévéré, Noëmie Lebret, Ludovic Mocochain, Speranta-Maria Popescu, Jordi Martinell, Rosa Doménech, Jean-Loup Rubino, Charles Gumiaux, Sophie Warny, Spyridon M. Bellas, Christian Gorini, François Bache, Marina Rabineau, Ferran Estrada

PII: S0264-8172(15)00048-3

DOI: 10.1016/j.marpetgeo.2015.02.016

Reference: JMPG 2148

To appear in: *Marine and Petroleum Geology*

Received Date: 29 July 2014

Revised Date: 9 February 2015

Accepted Date: 12 February 2015

Please cite this article as: Clauzon, G., Suc, J.-P., Couto, D.D., Jouannic, G., Melinte-Dobrinescu, M.C., Jolivet, L., Quillévéré, F., Lebret, N., Mocochain, L., Popescu, S.-M., Martinell, J., Doménech, R., Rubino, J.-L., Gumiaux, C., Warny, S., Bellas, S.M., Gorini, C., Bache, F., Rabineau, M., Estrada, F., New insights on the Sorbas Basin (SE Spain): the onshore reference of the Messinian Salinity Crisis, *Marine and Petroleum Geology* (2015), doi: 10.1016/j.marpetgeo.2015.02.016.

New insights on the Sorbas Basin (SE Spain): the onshore reference of the Messinian Salinity Crisis

Georges Clauzon[1*], Jean-Pierre Suc[2-3], Damien Do Couto[4], Gwénaël Jouannic[5], Mihaela Carmen Melinte-Dobrinescu[6], Laurent Jolivet[7], Frédéric Quillévéré[8], Noëmie Lebret[7], Ludovic Mocochain[2], Speranta-Maria Popescu[9], Jordi Martinell[10], Rosa Doménech[10], Jean-Loup Rubino[11], Charles Gumiaux[7], Sophie Warny[12], Spyridon M. Bellas[13], Christian Gorini[2-3], François Bache[14], Marina Rabineau[15], Ferran Estrada[16]

1, Aix-Marseille Université, CNRS, IRD, CEREGE UM34, 13545, Aix-en-Provence, France

* G. Clauzon died on March, 12, 2013

2, Sorbonne Universités, UPMC Univ. Paris 06, UMR 7193, Institut des Sciences de la Terre Paris (iSTeP), 75005 Paris, France

3, CNRS, UMR 7193, Institut des Sciences de la Terre Paris (iSTeP), 75005 Paris, France

4, Section of Earth and Environmental Sciences, University of Geneva, 13 rue des Maraîchers, CH-1205, Geneva, Switzerland

5, Cerema, DTer Est, Laboratoire Régional des Ponts et Chaussées de Nancy, 54510 Tomblaine, France

6, National Institute of Marine Geology and Geoecology, 23-25 Dimitrie Onciul street, P.O. Box 34-51, 70318 Bucharest, Romania

7, Université d'Orléans, ISTO, UMR 7327, 45071 Orléans, France

CNRS/INSU, ISTO, UMR 7327, 45071 Orléans, France

BRGM, ISTO, UMR 7327, BP 36009, 45060 Orléans, France

8, Université Lyon 1, Laboratoire de Géologie de Lyon, Terres, Planètes, Environnement, UMR 5276 CNRS, 27-43 boulevard du 11 Novembre 1918, 69622 Villeurbanne Cedex, France

9, GeoBioStratData.Consulting, 385 route du Mas Rillier, 69140 Rillieux la Pape, France

10, Departament d'Estratigrafia, Paleontologia i Geociències Marines, Facultat de Geologia, Universitat de Barcelona, c/Marti i Franqués s.n., 08028 Barcelona, Spain

11, TOTAL, TG/ISS, CSTTF, Avenue Laribeau, 64018 Pau Cedex, France

12, Department of Geology and Geophysics and Museum of Natural Science, Louisiana State University, Baton Rouge, LA 70803, USA

13, Ministry of Environment, Energy and Climate Change, Hellenic Republic, Directoriate of Petroleum Policy, Athens, Greece.

14, GNS Science, Ocean Exploration Section, P.O. BOX 30368, Lower Hutt 5040, New Zealand

15, Université de Bretagne Occidentale, IUEM, Domaines océaniques, UMR 6538 CNRS, 1 place Nicolas Copernic, 29280 Plouzané, France

16, Instituto de Ciencias del Mar de Barcelona, C.S.I.C., Passeig Marítim de la Barceloneta 37-49, 08003 Barcelona, Spain

Corresponding author: Jean-Pierre Suc, jeanpierre.suc@gmail.com, postal address: 385 route du Mas Rillier, 69140 Rillieux la Pape, France.

Abstract

The Sorbas Basin is the land reference of the Messinian Salinity Crisis (MSC) that affected the Mediterranean Sea in the latest Miocene. Its stratigraphy has been re-visited using calcareous nannofossils and planktonic foraminifers, which provide a reliable biostratigraphic frame and lead to particularly specify the relationships between the Sorbas and Zorreras members with Yesares evaporites.

The evaporites overlie a shallowing upward sequence ending with the deposition of the Reef Unit and Terminal Carbonate Complex (TCC) on the periphery of the basin. The reefal carbonates of the TCC are overlain by clastic deposits that are foreset beds of post-MSC Gilbert-type fan deltas developed on the northern edge of the basin. These sedimentary structures are separated from reefal carbonates and the Reef Unit by the Messinian Erosional Surface (MES). The various facies of the Sorbas Member have been correlated with the bottomset beds of the Gilbert-type fan deltas despite some differences in palaeobathymetry. In the southeastern periphery of the basin, the MES separates the Sorbas Member from the Yesares gypsums. In the central part of the basin, a hiatus characterizes the contact between these members. The Zorreras Member postdates the MSC and entirely belongs to Zanclean. Its white “Lago Mare” layers are lagoonal deposits, the fauna of which is confirmed to result from Mediterranean–Paratethys high sea-level exchange after the post-MSC marine reflooding of the Mediterranean Basin.

This study allows to re-assert the two-step scenario of the MSC (Clauzon et al., 1996) with the following events:

- at 5.971–5.600 Ma, minor sea-level fall resulting in the desiccation of this peripheral basin with secondary fluctuations;
- at 5.600–5.460 Ma, significant subaerial erosion (or lack of sedimentation) caused by the almost complete desiccation of the Mediterranean Sea;

- instantaneous marine reflooding, accepted at 5.460 Ma, followed by continuing sea-level rise.

Key-words: Messinian Salinity Crisis – Peripheral basin – Biostratigraphy – Sea-level changes – Erosion – Gilbert-type fan deltas.

1. Introduction

The Sorbas Basin (Fig. 1) has been known worldwide since the 1970's for its bearing on the scenarios of the Messinian Salinity Crisis (MSC) (Hsü et al., 1973). Extensive studies have been performed in this basin (e.g.: Dronkert, 1976, 1977; Ott d'Estevou and Montenat, 1990; Gautier et al., 1994; Martín and Braga, 1994; Clauzon et al., 1996; Roep et al., 1999; Riding et al., 1999; Krijgsman et al., 1999, 2001; Fortuin et al., 2000; Roveri et al., 2009), which is considered today as displaying the most relevant evidence of the crisis in the Mediterranean periphery (CIESM, 2008). The imprint of the following events which occurred from 6 to 5 Ma is preserved in the Sorbas Basin: (1) onset of the crisis as evidenced by the deposition of thick gypsums (Gautier et al., 1994; Krijgsman et al., 1999; Manzi et al., 2013), i.e. the 1st step of evaporitic sedimentation (Clauzon et al., 1996); (2) a diversified post-evaporitic sedimentation (Ott d'Estevou and Montenat, 1990; Dabrio and Polo, 1995; Roep et al., 1999, Martín-Suárez et al., 2000); its relationships with the events that occurred simultaneously in the central Mediterranean basins are controversial (Clauzon et al., 1996; Riding et al., 1998, 1999; Fortuin et al., 2000; Roveri et al., 2009); a Lago Mare episode (Civis, 1979; Ott d'Estevou and Montenat, 1990; Martín-Suárez et al., 2000; Do Couto et al., 2014b); and (3) the Zanclean marine incursion (Montenat and Ott d'Estevou, 1977).

Despite detailed stratigraphic descriptions of the basin (Ruegg, 1964; Dronkert, 1976; Ott d'Estevou and Montenat, 1990), numerous questions are still debated, as for example the significance of the "Lago Mare" deposits (Zorreras Member: Civis et al., 1979; Ott d'Estevou and Montenat, 1990; Martín-Suárez *et al*., 2000; Clauzon et al., 2005; Do Couto et al., 2014b). Except for important but local information, such as the occurrence of *Ceratolithus* cf. *acutus* in a crucial locality (Cortijo del Hoyo: Sánchez-Almazo, 1999), which has been published without information on the geographic location of the nannofossil-bearing locality

(Sánchez-Almazo et al., 1999; Braga et al., 2006), the post-evaporitic marine deposits of the Sorbas Basin lack reliable biostratigraphy, and hence accurate chronostratigraphy.

We revisited here the history of the Sorbas Basin based on new stratigraphic and geomorphological analyses. Our interpretation is supported by calcareous nannofossils and planktonic foraminifer data. Our data provide new constrains on the evolution of sea-level changes between 6 and 5 Ma.

2. Geological setting

The West-East trending Andalucian Sorbas Basin (Southeastern Spain; Fig. 1) is part of a mosaic of intramontane basins that formed above the exhumed metamorphic zones of the internal Betics during the Neogene (García-Dueñas *et al.*, 1992; Vissers et al., 1995; Johnson et al., 1997; Martínez-Martínez et al., 2002; Augier et al., 2005; Jolivet et al., 2006). The basin is thus surrounded by metamorphic basement units that form the Sierra de los Filabres to the North and the Sierra Alhamilla and Sierra Cabrera to the South (Fig. 1). The Sorbas Basin developed from the Serravallian to the Pliocene and subsidence maximum occurred during the Tortonian (Do Couto et al., 2014a). Following the deposition of continental conglomerates (considered as Tortonian: Ott d'Estevou and Montenat, 1990), an episode of rapid subsidence resulted in the deposition of Tortonian turbiditic sandstones (Ott d'Estevou and Montenat, 1990). The tectonic inversion of the basin, associated with a North-South compression that uplifted the basin, began near the Tortonian-Messinian boundary and is still active today (Weijermars et al., 1985; Sanz de Galdeano and Vera, 1992; Augier et al., 2005; Serpelloni et al., 2007). The basin became shallow-marine during the Messinian (Ott d'Estevou and Montenat, 1990; Do Couto et al., 2014a).

2.1. Lithostratigraphic and chronostratigraphic framework

Usually, the sedimentary filling of the Sorbas Basin is described as the succession of six nearly conformable lithological units that were deposited between the late Tortonian and the early Zanclean (Fig. 2). These include, in stratigraphic order, (1) the calcarenite of the Azagador Member (upper Tortonian), (2) the clays of the Lower Abad Member (lower Messinian), (3) the alternating clays and diatomites of the Upper Abad Member, (4) the thick gypsums alternating with clays of the Yesares Member especially at its top, (5) the limestone and clays of the Sorbas Member (limestone, called the Sorbas Limestone, is particularly thick below the village of Sorbas), and (6) the loams and pebbles of the Zorreras Member including three white chalky layers. The base of the Zanclean is placed either within the Zorreras Member (Ott d'Estevou and Montenat, 1990; Riding et al., 1998) or at the overlying marine coquina (Fortuin et al., 2000; Martín-Suárez et al., 2000; Roveri et al., 2009). On the edges of the basin, the Abad Member passes laterally to a thick coral Reef Unit whereas the Sorbas Member and, depending on authors, the upper part of the Yesares Member passes laterally to a carbonate and detritic unit called the Terminal Carbonate Complex (TCC) (Fig. 2). Based on the first attempts at precisely dating these members (planktonic foraminifers and magnetostratigraphy: Gautier et al., 1994; Krijgsman et al., 1999; planktonic foraminifers: Fortuin et al., 2000; mammals and magnetostratigraphy: Martín-Suárez et al., 2000; cyclostratigraphy: Roveri et al., 2009), the Abad, Yesares and Sorbas members together with most of the Zorreras Member and Reef Unit plus the TCC represent the Messinian Stage (Fig. 2).

Striking features in the Sorbas Basin include:

- (1) coral reefs at the periphery of the basin associated with the pre-MSC sea level (Esteban, 1979-1980; Ott d'Estevou et al., 1990; Martín and Braga, 1994; Braga and

Martín, 1996; Conesa, 1997; Martín et al., 1997; Cuevas Castell et al., 2007; Sánchez-Almazo et al., 2007; Bourillot et al., 2010b);

- (2) evaporites (gypsum) associated with almost complete desiccation (Ruegg, 1964; Dronkert, 1976; Rouchy, 1976; Ott d'Estevou and Montenat, 1990; Michalzik, 1996; Goubert et al., 2001);
- (3) evidence of erosion (Gautier et al., 1984; Riding et al., 1998, 1999; Braga et al., 2006; Roveri et al., 2009).

The first magnetostratigraphic studies of Messinian were performed in the Sorbas Basin and resulted in the time-calibration of the MSC (Gautier et al., 1994; Krijgsman et al., 1999; Martín-Suárez et al., 2000) and deposits astronomically tuned (Krijgsman et al., 1999, 2001; Sierro et al., 1997, 1999, 2001, 2003). The Sorbas Basin has been chronostratigraphically correlated with the Atlantic continuous sedimentary succession of the nearby Morocco (Gautier et al., 1994; Krijgsman et al., 2004; Krijgsman and Meijer, 2008).

The Sorbas Basin (Figs. 2 and 3) has provided the basis for three significantly different interpretations of the history of the MSC discussed during the last decade (Clauzon et al., 1996; Riding et al., 1998; Krijgsman et al., 1999). The debate has since been focussed on the end of the episode of reefal construction (i.e. the TCC), and on the geographic and chronologic location of the erosion relative to the MSC. This erosional phase has been placed by previous workers at different stratigraphic levels (Fig. 2): either (1) below the gypsum beds (Riding et al., 1999, 2000; Braga et al., 2006; Bourillot et al., 2010a), or (2) within the TCC and at the base of the Sorbas Member (Roveri et al., 2009), (3) in the upper part of the Zorreras Member (Gautier et al., 1994), (4) between the Sorbas and Zorreras members (Fortuin et al., 2000; Krijgsman et al., 2001; Aufgebauer and McCann, 2010).

2.2. Key agreements and disagreements: a review

Magnetostratigraphic studies performed by Gautier et al. (1994) and Krijgsman et al. (1999) are consistent and resulted in two well accepted chronostratigraphic data sets: the high-resolution cyclostratigraphy of the Abad Member (Krijgsman et al., 2001; Sierro et al., 2003), and the datation at 5.971 Ma of the lowermost gypsum (Fig. 2; Manzi et al., 2013). The stratigraphic correlation of the Upper Abad Member with the youngest coral reefs (Sierro et al., 1999, 2001), as observed at Cuesta de Cariatiz (Bourillot et al., 2010b), can also be considered as robust. The gypsum–clay alternations of the Yesares Member (Dronkert, 1976; Ott d'Estevou and Montenat, 1990) are well documented and interpreted in terms of precessional forcing (Krijgsman et al., 2001) or by a harmonic competition between uplift and erosion at the Gibraltar sill (Garcia-Castellanos and Villaseñor, 2011). It is widely considered that the clay layers that alternate with gypsum beds were deposited under full marine conditions being especially well established for the upper ones (Montenat et al., 1980; Lacour and Néraudeau, 2000; Saint-Martin et al., 2000; Goubert et al., 2001; Lacour et al., 2002; Néraudeau et al., 2002).

It is commonly accepted that the TCC, which was first defined as a reefal carbonate deposit delimited by two important erosional surfaces (Esteban, 1979-1980), overlies the Reef Unit. Esteban and Giner (1980) proposed that the two erosional phases were due to successive undated emergences (Fig. 4). Dabrio and Polo (1995) and Roep et al. (1998) expanded the definition of the TCC by including in it the overlying, mainly conglomeratic deposits (with an erosive base), and correlated them with the upper Sorbas Member, both deposited during high sea level (Fig. 4). Despite their mention of three erosional surfaces and regardless of the lack of age control, these authors proposed stratigraphic correlations between the periphery and the centre of the Sorbas Basin via a process of continuous sedimentation (Fig. 4). The option of continuous sedimentation in the coastal area of the Sorbas Basin is accepted by Conesa et al. (1999) and Cornée et al. (2004). Instead these authors proposed more complex relationships

between the periphery and the centre of the Sorbas Basin, in particular correlating the reefal carbonates plus the lowermost part of the clastic deposits with the Yesares Member (Fig. 4). Such a correlation was already suggested by Fortuin and Krijgsman (2003) (Fig. 4) who, however, recognized the occurrence of an erosional surface below the clastic deposits. A TCC extending up to the clastic deposits is also considered by Roveri et al. (2009) who attempted an astronomically tuned chronology by considering the absence of sedimentary gap at the same time as they located the Messinian Erosional Surface (MES) within the TCC between the reefal carbonates and the clastics (Fig. 4). Finally, Bourillot et al. (2010b) accepted the extended TCC recognizing a gap in sedimentation but only near the periphery of the Sorbas Basin (Fig. 4). To conclude, it is clear that some major differences exist in the interpretation of the detrital deposits that top the TCC. Some authors interpreted them as clinoform-shaped and prograding (Roveri et al., 2009; Bourillot et al., 2010b) whereas other interpreted them as flexured and tilted (Dabrio and Polo, 1995; Roep et al., 1998; Conesa et al., 1999).

Other disagreements concern the presence or absence of the MES in the Sorbas Basin and its stratigraphic location (Fig. 2). The first reference to the MES in this basin was by Gautier et al. (1994) who placed it at the base of the clastic sediments (conglomerates, sands) overlying the marine coquina of the uppermost Zorreras Member (MES 1 in Figure 2). An older stratigraphic position has since been proposed (Roveri et al., 2009). Although these authors noted that the surface is poorly expressed, they located it within the TCC, at the topmost of the Yesares Member (MES 2 in Figure 2). The lowermost stratigraphic location was suggested by Riding et al. (1999, 2000) who placed the surface at the base of the Yesares evaporitic Member (MES 3 in Figure 2). This interpretation, accepted by Bourillot et al. (2010b), had been earlier opposed by Fortuin et al. (2000). Ott d'Estevou and Montenat (1990) proposed a progressive passage from the Messinian to the Zanclean, accepted by Fortuin et al. (2000), Cornée et al. (2004), and Aufgebauer and McCann (2010). Resolving

this debate is crucial if one is to soundly reconstitute the Messinian history of the Sorbas Basin. At this time it is necessary to reach a consensus on the age of the Sorbas and Zorreras members and on the interpretation of sedimentary succession in the Sorbas Basin in terms of sea-level changes.

As another item of discussion, the Zorreras Member includes three white chalky layers (Fig. 2) that are usually referred to the so-called “Lago Mare”, because they contain the ostracod *Cyprideis pannonica* (Civis et al., 1979) and a mollusc fauna composed of dreissenids and limnocardiids (Ott d’Estevou et al., 1990). The “Lago Mare” has often been set up as a single sequence (with a chronostratigraphic sense) ending the MSC (Cita and Colombo, 1979; Orszag-Sperber, 2006). However, Clauzon et al. (2005) proposed the occurrence of three “Lago Mare” events between 6 and 5 Ma, two of which are considered associated with distinct high sea levels (Messinian and Zanclean, respectively). The environmental significance of the “Lago Mare” deposits in the Sorbas Basin has been specified (Do Couto et al., 2014b) but its stratigraphic sense needs to be clarified.

3. Method

The approach on which this study is based in determining wether the base of the deposits associated with the post-MSC marine reflooding of the Mediterranean is an erosional surface and which sedimentary features characterize them. Therefore, we performed field study based on stratigraphic and geomorphological observations as well as palaeontological analyses to characterize chronostratigraphy.

Calcareous nannofossils were analysed to date the clayey sediments, being best suited for the stratigraphy of shallow marine sediments and their long distance correlations. Smear slides were prepared directly from the untreated samples to retain the original sample

composition. The analysis of calcareous nannofossils was performed using a light polarizing microscope at x1600 magnification. Taxonomic identification followed Perch-Nielsen (1985) and Young (1998). A very careful analysis of each sample was performed, i.e. examining more than 50 fields of view, in order to find rare specimens, such as for example *Ceratolithus acutus* and *Triquetrorhabdulus rugosus*, which are important index species of the Messinian – Zanclean boundary interval (Raffi et al., 2006). Figure 5 shows all the key species considered in this work and their chronostratigraphic range within the corresponding NN (Neogene Nannoplankton) Zonation (Martini, 1971; Berggren et al., 1995; Raffi et al., 2006). Seventy samples were studied (Table 2). Preservation was generally moderate, with about 25-30 species showing overgrowth and/or dissolution. Reworked nannofossils were frequent, being mostly composed of Cretaceous, Paleogene and a few pre-MSC Neogene species. The studied samples are from the topmost layers of the Yesares Member, the uppermost TCC, the Sorbas and the Zorreras members (Fig. 2).

We searched for planktonic foraminifers in several outcrops in the area of La Cumbre (Fig. 6). Samples were wet-sieved over 250 μm, 125 μm and 63 μm screens. Specimens, which exhibit moderate preservation, were picked under a binocular microscope and identified following the taxonomic concepts and nomenclature of Kennett and Srinivasan (1983). Figure 5 shows the planktonic foraminiferal key species considered and their chronologic range (Lourens et al., 2005).

In this paper, the ages of the lowest and highest occurrences of the considered species are those published by Lourens et al. (2005) for planktonic foraminifers and Raffi et al. (2006) for calcareous nannofossils. As they have been established in long sedimentary records in line with continuous $\delta^{18}O$ curves astrochronologically tuned, such ages have been provided with a very high precision and without uncertainty interval. For some species, two ages are proposed

originating from different sites: we opted for the oldest one in the case of a lowest occurrence, and for the youngest one in the case of a highest occurrence.

Many samples have been prepared for palynological analyses (pollen grains, dinoflagellate cysts). Unfortunately, all samples were barren.

This methodology has been successfuly applied around the Mediterranea Basin (Clauzon et al., 2005; Melinte-Dobrinescu et al., 2009; Bache et al., 2012), and several Gilbert-type fan deltas have been distinguished above the MES (Bache et al., 2012). In many places around the Mediterranean Basin, Gilbert-type fan deltas document the complete reflooding of the Mediterranean Basin after the MSC (Clauzon, 1990; Bache et al., 2012). Gilbert-type fan deltas are sedimentary features that require some accommodation to develop. Within the Mediterranean peripheral basins, accommodation resulted from intense fluvial erosion followed by rapid marine reflooding. These unique deltas exhibit the following characteristics (Clauzon, 1990):

- (1) the MES bounding the submarine unit at its base;
- (2) frequent debris flows (Breda et al., 2007) made of reworked blocks including elements from the peripheral Messinian evaporites immediately overlying the MES (Bache et al., 2012);
- (3) a prograding submarine part (clayey bottomset beds and conglomeratic to sandy foreset beds, the sedimentary dips of which may reach 30-35°) and an aggrading subaerial part (conglomeratic to sandy, almost horizontal topset beds often affected by surface alteration);
- (4) diachrony of the marine-continental transition at the contact between the foreset and topset beds, showing the retreat of the shoreline during the progradation of the Gilbert-type fan delta;

- (5) the abandonment surface bounding the deltaic system at the top; the abandonment surface indicates the end of the aggradation which occurred at the Late Pliocene coolings and the following Quaternary glacials (Clauzon, 1996). At places where erosion was weaker, such as interfluves or locations far from the valley axis, the contact between the Messinian peripheral evaporites or older rocks and the post-MSC deltaic deposits may appear conformable. However, an unconformity, called the Messinian Discontinuity, separates them (see for examples; Melinte-Dobrinescu et al., 2009; El Euch – El Koundi et al., 2009). The geological map from Ott d'Estevou (1990) was used to locate the stratigraphic members and the main sections studied in this work (Fig. 3).

At places where erosion was weaker, such as interfluves or locations far from the valley axis, the contact between the Messinian peripheral evaporites or older rocks and the post-MSC deltaic deposits may appear conformable. However, an unconformity, called the Messinian Discontinuity, separates them (see for examples; Melinte-Dobrinescu et al., 2009; El Euch – El Koundi et al., 2009). The geological map from Ott d'Estevou (1990) was used to locate the stratigraphic members and the main sections studied in this work (Fig. 3).

4. Field observations and palaeontological results: palaeoenvironmental inferences and age assignments

We provide our field observations in association with the micropalaeontological content and hence the biostratigraphic assignment of the concerned sections in the geographic parts of the Sorbas Basin.

4.1. The northern edge of the basin: Cariatiz, Góchar and Moras areas

Cuesta de Cariatiz is a propitious place (Figs. 3 and 6; Table 1) for studying the TCC (Fig. 7A and B), especially its upper part. This section has been interpreted as corresponding to a fluvial deposit (Roveri et al., 2009; Bourillot et al., 2010b). The downlapping sedimentary architecture that it exhibits, with great sedimentary dip of sandy–conglomeratic beds (32° southward) and lateral imbrications with marine microplankton-bearing clays (Fig. 7E; Table 2a) indicates a subaqueous deltaic prograding sedimentation. This is characteristic of Gilbert-type fan deltas, an interpretation also supported by an almost horizontal transition to aggrading continental loams (Fig. 7E), which corresponds to the marine-continental transition. The base of this Gilbert-type fan delta overlies the reefal carbonates of the TCC or their alterated surface with a sharp erosional contact (Fig. 7A, C and D). This erosional contact is more marked than previously reported by Bourillot et al. (2010b). The reefal carbonates are also nested within the Reef Unit, probably through the older erosional contact indicated by Esteban (1979-1980), Dabrio and Polo (1995) and Roep et al. (1998) (Fig. 7A and B). Two samples from the bottomset beds (Fig. 7A and E) yielded a diversified assemblage of calcareous nannofossils (Table 2a) which, based on the co-occurrence of *Ceratolithus acutus* and *Triquetrorhabdulus rugosus* (Fig. 5), belongs to the Subzone NN12b.

Similar observations have been made in the area of Góchar and Moras (Figs. 3 and 6; Table 1) regarding the top of the Reef Unit, the detritic upper TCC described by Conesa (1997) and the Zorreras Member. In fact, field work shows that two coalescing branches of a Gilbert-type fan delta originated respectively from Manantial de los Charcones (1.6 km northward Góchar) and immediately northward of Moras (Fig. 6). They are both nested within the Reef Unit, which culminates at the altitude of 600 m. At these locations, the erosional contact above the Reef Unit is at the altitudes of 479 m and 461 m, respectively (Fig. 8A, B, D and E). At Moras, the bottomset beds exposed just below the marine-continental transition (Fig. 8D),

yielded a diversified assemblage of calcareous nannofossils including *C. acutus* and *T. rugosus* (Table 2a), which characterizes Subzone NN12b (Fig. 5). A sample from Manantial de los Charcones provided an assemblage of calcareous nannofossils (Fig. 8A and B) with *T. rugosus* (Table 2a). Because of the absence of *Ceratolithus acutus* and *Discoaster quinqueramus*, this sample can be ascribed to Subzone NN12a (Fig. 5). There, eroded colonies of *Porites* are widely bored by mollucs (bivalves: ichnogenus *Gastrochaenolites*; Fig. 8C). At Moras, the marine-continental transition of the Gilbert-type fan delta, characterized by the presence of small specimens of echinoids, is located at 475 m a.s.l. (Figs. 8D-F). Downstream within the Rambla de Góchar, the conglomeratic and sandy topset beds with cross-bedded sedimentation are progressively replaced by red loams including chalky white layers and a bivalve coquina. Southward of Góchar, the completeness of the Gilbert-type fan delta allows observation of flat to weakly inclined abandonment surfaces preserved for a 1.5 km distance from about 455 m to 435 m a.s.l. (Fig. 8G), the Zorreras summit (at an altitude 410 m; Fig. 6) being the ultimate preserved evidence of this surface to the South.

4.2. The central part of the basin: Sorbas – Zorreras area

This area allows to observe the Yesares and Sorbas members in several localities and their stratigraphic relationships in some of them.

The base of the Yesares Member is dated at 5.971 Ma (Manzi et al., 2013). The age of its top is estimated at 5.600 Ma based on the proposed precession-tuned sixteen gypsum-clay alternations by Roveri et al. (2009) and Manzi et al. (2013). In the Peñon Díaz quarry (Figs. 3 and 6; Table 1), clays of cycle 10 from Roveri et al. (2009), located at about 120 m in thickness above the base of the Yesares Member, contain marine fossils, including foraminifers unfortunately devoid of biostratigraphic significance (Ott d'Estevou and

Montenat, 1990; Goubert et al., 2001). According to the Roveri et al. (2009)'s cyclostratigraphy, these clays would be ca. 5.75 Ma old. We found a calcareous nannoplankton assemblage in these clays containing *Triquetrorhabdulus rugosus* in two samples (Table 2a). In the absence of *Nicklithus amplificus*, these clays can be ascribed to Subzone NN11d (*ca*. 5.939 – 5.540 Ma; Fig. 6; Raffi et al., 2006).

A section through the Yesares Member can also be observed within the famous karstic Cuevas de Sorbas (Figs. 3 and 6; Table 1; Calaforra and Pulido-Bosch, 2003). There, indurated marls alternating with gypsum showed to us some specimens of the bivalves *Arca noae* and *Cerastoderma edule*. *Arca noae* is an epifaunal species that lives attached to rocks or shells through the bissus, from the intertidal zone in estuarine and inner shelf environments of up to more than 100 m water depth (Poppe and Goto, 1993). The presence of a specimen with the shell closed could indicate that transport before burial was negligible. *Cerastoderma edule* occurs with the valves attached and closed. This is an infaunal bivalve that lived slightly buried in sand or mud, from the intertidal zone to a few metres water depth. This species especially favours areas with some fresh water input (Poppe and Goto, 1993). The specimen position within the sediment suggests that they are in life position, and therefore would have not been transported. This impoverished marine malacofauna gives an idea about the poor life conditions at the time of gypsum deposition.

Cortijo del Hoyo (Figs. 3 and 6; Table 1) is a locality where the stratigraphic relationships between the Yesares and Sorbas members can be observed. The clays of the Sorbas Member are at the same altitude as the Yesares gypsums and form a continuous cliff with them (Fig. 9A and C), which could indicate a lateral passage in contradiction with their usually described conformable vertical succession (Fig. 2; Ott d'Estevou and Montenat, 1990; Riding et al., 1999; Fortuin et al., 2000; Krijgsman et al., 2001; Braga et al., 2006; Roveri et al., 2009). Calcareous nannofossils have been recovered from two sections (Table 2a). Samples 1 to 24

cover the interval from the uppermost clays associated with the gypsums of the Yesares Member up to the sandstones overlying the clays of the Sorbas Member (Fig. 9A and B). Sample 1 provides several well-preserved specimens of *Discoaster quinqueramus* (last occurrence at 5.540 Ma; Fig. 5; Raffi et al., 2006), suggesting that they are not reworked (Table 2a; Pl. 1, Figs. 5 and 6). Samples 2 and 3 are barren. *Ceratolithus acutus* (first occurrence at 5.345 Ma; Fig. 5; Raffi et al., 2006) is present in the six following samples (Pl. 1, Fig. 1; Table 2a). *Triquetrorhabdulus rugosus* is continuously recorded throughout (Table 2a). This nannoplankton succession may be considered as indicative of Subzones NN11d and NN12b without Subzone NN12a (Fig. 5). There, in the absence of any fault between the Yesares and Sorbas members, it is concluded that they are separated by an erosional surface (Fig. 9A and B). The presence of gypsum at the base of the cliff some hundreds of metres further to the NW reinforces this inference that is also supported by the presence of *C. acutus* in samples 26 and 27 (Table 2a) taken in the clays at a lower altitude (Fig. 9A and B). Consistently, *Ceratolithus* cf. *acutus* was mentioned by Sánchez-Almazo (1999) in three samples from the same clays as our samples 26 and 27 in a nearby section located 700 m westward of our section, a result that was not used from the biostratigraphic viewpoint. There, the marine-continental transition has been observed at the contact between the clays and the overlying sandstones where some small echinoids have been recorded (Fig. 9).

The clays of the Sorbas Member are also exposed at Corral de Juan Cipriano (Figs. 3, 6 and 9D; Table 1) where *Ceratolithus acutus* has not been recorded (Table 2a). At this locality, the marine-continental transition locates at the contact between the Sorbas and the Zorreras members, the latter showing its characteristic white clayey layers (Fig. 9D) as observed at Cuesta de Cariatiz (Fig. 7E).

Another place where the Sorbas and Yesares members can be observed, again at the same altitude, is the area of the Panoramic Viewpoint (Figs. 3, 6, 10; Table 1). *Triquetrorhabdulus*

rugosus has been recorded in eleven samples, associated with *Ceratolithus acutus* recorded in samples 5, 12, 19 and 20 (Table 2b). The same biostratigraphic markers have also been separately recorded in samples 23-24 (*T. rugosus*) and 26 (*C. acutus*), respectively, close to the Yesares gypsum (Fig. 10, Table 2b). This nannoplankton succession may be considered as indicative of Subzones NN12a and NN12b (Fig. 5). There, the contact between the uppermost gypsum and overlying clays containing *C. acutus* is erosional.

Roep et al. (1998) demonstrated the existence of lateral transitions between the various facies of the Sorbas Member, which were interpreted as resulting from minor sea-level variations preceding the Mediterranean drawdown at the peak of the MSC. Indeed, lateral changes between the prevalent facies, carbonates (i.e. the Sorbas Limestone) and clays, are observed around Sorbas, particularly at Cortijo de Paco el Americano (Figs. 3, 6, 11A and B; Table 1) and near the Hostal Sorbas (Figs. 3, 6, 11D; Table 1). Three samples have been taken in thin clay intercalations within the Sorbas Limestone on the right bank of the Río Aguas (Figs. 3, 6, 11B and C). The calcareous nannofossil assemblage contains both *Ceratolithus acutus* and *Triquetrorhabdulus rugosus* (Table 2b) allowing the Sorbas Limestone to be ascribed to Subzone NN12b (Fig. 5; Raffi et al., 2006). A similar result was obtained in samples selected from the section near the Hostal Sorbas (Fig. 11D; Table 2b).

In the Zorreras area (Figs. 3 and 6), clays of the Sorbas Member are laminated (Fig. 12A and B), overlying the Sorbas Limestone at Cortijo Marchalien La Gorda (Table 1). They are equivalent to those found at El Marchalico (1.5 km to the East in the Las Lomas area; Fig. 6) that provided many specimens of the marine fish *Aphanius crassicaudus* (Gaudant and Ott d'Estevou, 1985). This monospecific ichtyofauna is described as representative of an estuarian palaeoenvironment (Gaudant and Ott d'Estevou, 1985; Ott d'Estevou and Montenat, 1990). At Cortijo Marchalien La Gorda, these levels provided a calcareous nannoplankton assemblage (Fig. 12B and C), which, according to the co-occurrence of *Ceratolithus acutus*

and *Triquetrorhabdulus rugosus* (Table 2c), belongs to Subzone NN12b (Fig. 5; Raffi et al., 2006). In this section, the uppermost record of *C. acutus* is located just below the lowermost white chalky layer of the Zorreras Member (Fig. 12A and C; Table 2c). There, the marine-continental transition is marked by a thin red clayey bed (Fig. 12C).

The Zorreras Member is mostly known because it includes three white chalky layers (Fig. 13A to D), which are thought to have a lagoonal origin because of the presence of ostracods, charophyte oogonia and molluscs. The mollusc fauna is composed of dreissenids (*Dreissena* mostly) and limnocardiids (*Limnocardium*, *Prosodacna*, *Pseudocatillus*) (Ott d'Estevou et al., 1990) both of Paratethyan origin. The ostracod fauna includes *Cyprideis pannonica pseudoagrigentina* (Civis et al., 1979) (= *C. agrigentina*; Roep and Van Harten, 1979), a species described from the Messinian in Sicily (Decima, 1964; Colalongo, 1968), along with *Loxoconcha djaffarovi*, *Maeotocythere* (= *Euxinocythere*) *preabaquana*, and *Tyrrhenocythere pontica* (Roep and Van Harten, 1979). Most of these species are considered Paratethyan invasive species (Gliozzi et al., 2007). Such a biofacies was thus understood as representative of the "Lago Mare" (Roep et al., 1998), i.e. the *Loxoconcha djaffarovi* Zone of Carbonnel (1978), a concept still used (Gliozzi et al., 2006) despite the doubts concerning its stratigraphic value (Guernet, 2005), its origin (Clauzon et al., 2005) and its environmental significance (Riding et al., 1998). A fruitless search for nannofossils and dinoflagellate cysts has been performed on the white layers, where only the coastal foraminifers *Ammonia beccarii* and *Elphidium* sp. have been recorded. The loams and clays of the lower part of the Zorreras Hill (Figs. 3, 6, 13B; Table 1) exhibit reverse palaeomagnetism referred to Chron C3r (Gautier et al., 1994; Martín-Suárez et al., 2000). Martín-Suárez et al. (2000) place the lower two thirds of this section in the latest Messinian on the basis of a mammal fauna.

The base of the Zorreras section (Figs. 3 and 6; Table 1) is composed of silts (Fig. 13A and B) where we found fragments of epifaunal regular echinoids (plates and spines), cirripeds and

some specimens of the gastropod *Epitonium depressicosta* (Fig. 13E), a species only known from the Lower Pliocene of the Mediterranean (Landau et al., 2006). The bed that yielded echinoids corresponds to the marine-continental transition as mentioned above at Cortijo Marchalien La Gorda, Cortijo del Hoyo and Moras.

In the upper part of the Zorreras section just underlying the pebble zone (Fig. 13B), there is a 25 cm thick coquina made of bivalves arranged in pavement (Fig. 13F and G). This malacofauna was described and ascribed to the Pliocene by Montenat and Ott d'Estevou (1977). It was revisited for the work presented here. The base of the coquina (15 cm thick) is dominated by *Ostrea lamellosa* with calcitic skeletons (Fig. 13F). We observed both complete specimens and free valves are seen in the level, and the skeletal arrangement tends to be planar, forming a pavement composed of one-two shells. The shells were occasionally drilled, and the ichnogenera *Entobia* (produced by sponges) and *Caulostrepsis* (produced by annelids) have been identified. *Ostrea lamellosa* is an epifaunal cementing and euryhaline species that usually lives in monospecific banks. The top of the coquina consists of a pavement of infaunal bivalves represented by internal molds of average size about 7-8 cm in diameter umbonopaleal (Fig. 13G). The aragonite shells were dissolved by diagenetic processes, thereby hampering the taxonomic identification. Nevertheless, the dominant presence of veneroids (*Diplodonta rotundata*, *Pelecyora* aff. *brocchii*, *Dosinia exoleta*) and tellinids is clear. All these taxa bear smooth valves and are infaunal. Some *Ostrea lamellosa* shells have been observed and one occasional pectinid mold, both epifaunal taxa. The molds mostly correspond to closed valves and are arranged nearly parallel to the stratification plane. Measures taken randomly over an area of 1.5 m^2 do not indicate any preferred orientation of the fossils. It is noticeable that diagenetic processes of compaction have caused an umbonopaleal shift of around 1 cm between the valves of many specimens. This coquina could be interpreted as the result of two specific stormy episodes in a coastal environment,

below the lowtide level. The first one would have brought the oyster shells from a very close location. This episode was most likely followed by a period of sedimentation and installation of an infaunal community. Finally, a second stormy episode may have eroded the sea-bed and washed away the fine sediment. Bivalves were not transported a long distance, because the valves are held together and shells are closed. The scarce incidence of bioerosion in the oysters, and their relative thinness, concur with hypohaline environmental conditions, linked to the proximity of continental fresh waters. Montenat and Ott d'Estevou (1977) cited up to 22 different taxa in this coquina, including both epifaunal and infaunal forms, which have not been fully recognized at the outcrop visited. In addition, these authors also indicate the presence of a *Calyptraea* sp. (naticid gastropod), which has not been identified at this time. This coquina level can be followed along the red hills made of the Zorreras Member deposits up to the uppermost part of El Cerro Colorado (Figs. 3) and the top of La Cerrada hills in the Cuesta de Cariatiz area (Figs. 6). In the latter localities, the coquina only contains *Ostrea* shells.

4.3. The southwestern edge of the basin: La Cumbre and Los Molinos de Río Aguas areas

In the southern part of the Sorbas Basin, grey clays are observed sandwiched between the Sorbas Limestone (Sorbas Member) and sandstones of the Zorreras Member (Fig. 14A). At La Cumbre (Figs. 3, 6 and 14B; Table 1), these clays are topped with a coquina rich in *Ostrea* and Pectinidae, which locally marks the marine-continental transition (Fig. 14C and D). Their nannoplankton assemblage (Table 2c) contains *Ceratolithus acutus* (Pl. 1, Figs. 2 and 3) and *Triquetrorhabdulus rugosus* (Pl. 1, Fig. 7) indicating Subzone NN12b (Fig. 5; Raffi et al., 2006). At the 13th Congress of the Regional Committee on Mediterranean Neogene Stratigraphy (Naples, Sept. 2009), F.J. Sierro informed one of us (J.-P.S.) that he unexpectedly recorded *Globorotalia margaritae* in a sample from sediments immediately

underlying the Zorreras Member in the area of La Cumbre. This information led us to ask F.J. Sierro to search for foraminifers in our samples containing *C. acutus* in this area: "a consistent assemblage characteristic of shallow waters with abundant subtropical planktonic specimens" was found in two of these samples (F.J. Sierro, *in litteris*: Jan. 20, 2010). This result encouraged us to perform a systematic investigation of the clays sandwiched between the Sorbas Limestone and Zorreras Member near the Cerro de Juan Contrera (Figs. 3, 6 and 14B; Table 1), which have been sampled in several points (Fig. 14B, E and F). Some of them contain *T. rugosus* and *C. acutus* (sample 2) or only *T. rugosus* (samples 3 and 4) (Table 2c). Most of them yielded diversified assemblages of planktonic foraminifers, including *Sphaeroidinellopsis seminulina* (sample 2), *Globoturborotalita nepenthes* (samples 1, 2, 3 and 6; Pl. 2, Fig. 2 and b) and *Hirsutella* (*Globorotalia*) *margaritae* (samples 4 and 6; Pl. 2, Fig. 1a, b and c) (Table 3). This microplankton assemblage (calcareous nannofossils and foraminifers) dates the clays overlying the Sorbas Limestone between 5.345 and 5.279 Ma with respect to associated *T. rugosus* and *C. acutus* (Fig. 5; Raffi et al., 2006). In the nearby Cerro Quemado (Fig. 6), similar clays studied by Ott d'Estevou et al. (1990) yielded benthic and planktonic foraminifers, including *Globigerinoides emeisi*, a species ranging from the Late Miocene to the Pliocene (Bolli, 1966), which is in agreement with the age proposed above. At Barranco del Infierno (Figs. 3 and 6; Table 1), similar clays provided an almost identical calcareous nannoplankton assemblage including *C. acutus* and *T. rugosus* (Table 2c). In a last locality, Torcales del Pocico (Figs. 3 and 6; Table 1), the Sorbas Limestone was barren in nannofossils while the overlying clays yielded specimens of *C. acutus* and *T. rugosus* (Table 2c), supporting the biostratigraphic ascription.

At Los Molinos de Río Aguas (Figs. 3 and 6; Table 1), the Sorbas – Carboneras road crosses the gypsum bar at a pass (Fig. 15A, B and C). At the pass, abundant large and disconnected blocks of gypsum are wrapped within an astructured heterogeneous matrix composed of small

fragments and rounded pebbles of various clays, marls, where some small clasts originating from sierras are also included (Fig. 15D and E). Such a heterogeneous and heterometric material is obviously reworked.

5. Extended interpretation

We follow the chronology of Bache et al. (2012) (Fig. 5) who proposed the almost complete desiccation of the Mediterranean at about 5.6 Ma, its partial slow reflooding between *ca*. 5.5 and 5.46 Ma, and its instantaneous catastrophic reflooding at 5.46 Ma (i.e. the "Zanclean Deluge"). This event was followed by a continuous rise of the Mediterranean sea-level in connection with the global sea-level rise occurring up to 5.332 Ma as a response to ice melting (Haq et al., 1987; Miller et al., 2011).

5.1. Nature and age of the erosional surfaces

According to the nannofossil assemblage ascribed to Subzone NN12b recorded in its bottomset beds (Table 2a), the Cariatiz Gilbert-type fan delta developed during the latest Messinian and early Zanclean, mostly after 5.345 Ma (Fig. 5). Accordingly, we interpret the underlying erosional surface as the MES, which is sandwiched between deposits preceding the peak of the MSC and the first one following it (Fig. 7A, C and D). The Moras Gilbert-type fan delta has the same biozonal age (Subzone NN12a) as the Gilbert-type fan delta of Cuesta de Cariatiz. The erosional contact at the base of Gilbert-type fan delta deposits must also be considered as the MES (Fig. 8D and E). At Manantial de los Charcones, the sample ascribed to Subzone NN12a (Table 2a) immediately overlies the same erosional surface that we refer to the MES (Fig. 8A and B). As a consequence of these biostratigraphic ages, the upper part of the TCC (i.e. its most detritic part with rounded pebbles and sands) must be interpreted as

corresponding to latest Messinian – earliest Zanclean Gilbert-type fan deltas[1] separated from the Reef Unit by the MES.

The Messinian subaerial erosion did not impact the central area of the Sorbas Basin where the Sorbas Member has been commonly regarded as overlying conformably the Yesares Member. This is particularly true in the well-known Río Aguas section (37° 5' 23.6" N, 2° 6' 57.7" W; Fig. 16A). However, we consider that a ~200 kyrs long gap in sedimentation affected the central part of the Sorbas Basin, as suggested by biostratigraphic data from the topmost Yesares clays (*Discoaster quinqueramus* recorded at Cortijo del Hoyo: Table 2a) and from the Sorbas Limestone which yielded *Ceratolithus acutus* (Table 2b). According to Raffi et al. (2006), *D. quinqueramus* became extinct at 5.540 Ma while *C. acutus* appeared at 5.345 Ma (Fig. 6). Such a gap in sedimentation, that was called the Messinian Discontinuity in a similar sedimentary context (Melinte-Dobrinescu et al., 2009), is time-equivalent of the Messinian subaerial erosion. The best example of the Messinian Discontinuity is illustrated in the nearby Vera Basin in the famous Cuevas del Almanzora section (Cita et al., 1980; Clauzon, 1980).

To the Southeast, in the area of Cortijo del Hoyo and of the Panoramic Viewpoint (Figs. 3 and 6), the contact between the sediments of the Sorbas Member and the gypsum-clay alternations of the Yesares Member is erosional again, the former being nested within the latter (Figs. 9A-C and 10). There, biostratigraphy which mostly refers the clays of the Sorbas Member to the Subzone NN12b implies that the erosional surface is the MES. The re-appearance of erosion in the southeastern part of the basin suggests that the Messinian Río Aguas had to cut within the gypsum member.

[1] These Gilbert-type fan deltas have been first interpreted as pre-dating the peak of the MSC (Clauzon et al., 2008). This interpretation has been modified when nannofossil assemblage of their bottomset beds provided *Ceratolithus acutus* in several places (Clauzon et al., 2009).

It was thus crucial to evaluate where was located the Messinian valley used by the palaeo Río Aguas to exit the Sorbas Basin? At the pass of Los Molinos de Río Aguas, there is a palaeo-valley morphology that was probably exhumed as a result of the uplift of the southern edge of the basin Fig. 15A-C). According to its vicinity with the places (Cortijo del Hoyo, Panoramic Viewpoint) where the Messinian erosion was observed to have affected the gypsums (Fig. 3), this abandoned valley is a good candidate as the Messinian valley of the Río Aguas. This assumption is also supported by the occurrence of reworked deposits, that we interpret as a debris flow, which moulded the morphology of the palaeo-valley (Fig. 15C) prior to deposition of well-dated clays (Panoramic Viewpoint) just upstream the palaeo-valley (Fig. 15C). Such debris flow deposits are frequent on the MES around the Mediterranean Basin where they sign the post-crisis marine reflooding (Breda et al., 2007; Bache et al., 2012; Do Couto et al., 2014b). We thus consider that this uplifted palaeo-valley is the remaining Messinian valley of the Río Aguas at its outlet from the Sorbas Basin in the direction of the almost completely desiccated Mediterranean Basin (Fig. 15A, B and C). This palaeo-valley was also the gateway used later by marine waters to re-invade the Sorbas Basin at the time of the Mediterranean reflooding after the MSC.

We interpret the major erosion observed to the North and South-East of the Sorbas Basin as caused by fluvial cutting in response to the huge drop of the Mediterranean Sea level which is considered to have occurred at 5.600 Ma (Clauzon et al., 1996) and to have continued up to 5.460 Ma (Bache et al., 2012).

A previous weak erosional phase is testified by the contact between the reefal carbonates and the Reef Unit (Fig. 7A and B; Esteban, 1979-1980; Dabrio and Polo, 1995; Roep et al., 1998). It corresponds to a slight relative sea-level drop that we correlate with the deposition of the almost massive gypsums, i.e. between 5.971 and 5.800 Ma (Figs. 17 and 18). This cutting should have occurred in a subaerial context.

5.2. Age of the post-evaporitic units

This detailed study shows that the Sorbas Member was deposited after the marine reflooding that ended the MSC and it is separated from the Yesares Member by the MES. As in many places, we have established that both its laterally equivalent carbonate and clayey layers belong to the nannoplankton Subzone NN12b, pointing out the return of marine waters after the MSC. Accordingly, the Sorbas Member may be understood as the equivalent towards the South of the foreset and bottomset beds of the Góchar – Moras and Cariatiz Gilbert-type fan deltas. Differentiation within the Sorbas Member results from differences in bathymetry and its semi-enclosed palaeogeographical context (Martín et al., 1999: fig. 5E). In such a context, the Sorbas Limestone was deposited on a relatively higher topography closer to shoreline than the basinal clays. The fossil content indicates that the laminated clays were deposited in slightly deeper conditions than the Sorbas Limestone. For this reason, they are labelled as 'i' in the modified geological map with respect to that of Ott d'Estevou (1990) (Fig. 3). Sedimentation of the Sorbas Member is thus considered to have started at 5.460 Ma (the age of the marine reflooding of the Mediterranean: Bache et al., 2012) and its uppermost part could be of Pliocene age.

In the area of Cuesta de Cariatiz, the Zorreras Member (with its characteristic lowermost chalky white layer) immediately overlies the subaqueous part (foreset and bottomset beds) of the Gilbert-type fan delta and thus constitutes its topset beds. At the Zorreras Hill, the Zorreras Member (with its three characteristic chalky white layers) overlies the laminated clays of the Sorbas Member. It is the southern extension of the alluvial deposits equivalent to the topset beds of the Gilbert-type fan deltas. Considering (1) the above mentioned presence of the nannofossils *Ceratolithus acutus* and *Triquetrorhabdulus rugosus* (highest occurrence at 5.279 Ma; Fig. 5) in samples located just below the lowermost white chalky layer in several

localities (Cuesta de Cariatiz, Hostal Sorbas, Cortijo Marchalien la Gorda), and (2) the necessary time for sediments to prograde, we consider that the whole Zorreras Member is earliest Pliocene. The presence of *Epitonium depressicosta* in the lowermost beds of the Zorreras section is consistent with the proposed age for the whole Zorreras Member.

5.3. Mode of sedimentation above the Messinian Erosional Surface

The first evidence of marine reflooding is illustrated by the borings made by saxicavous mollusc within the *Porites* colonies impacted by the Messinian erosion (Fig. 8C). The Gilbert-type fan deltas are well exposed in three places (Cuesta de Cariatiz, Moras and Góchar) and show prograding submarine sediments (foreset and bottomset beds) toward the central part of the Sorbas Basin overlain by the aggrading topset beds which refer to the Zorreras Member. However, they should have a relatively slight space extension toward the basin (Fig. 3).

The distinct course of the modern Río Aguas in crossing the gypsum bar (Fig. 15A and B) results from a peri-Mediterranean frequent phenomenon linked to the post-MSC marine reflooding and sedimentary infilling by Gilbert-type fan deltas, called “aggradation epigenesis” (Fig. 19). This process, identified and described by Clauzon (1996), results from the succession of a double huge variation in sea level in the Mediterranean Basin (*ca*. 1500 m of sea-level drop and the following reflooding) and a long relatively stable high stand in sea level during the Early Pliocene (Haq et al., 1987; Miller et al., 2011). Indeed, when the Zanclean ria (i.e. the Messinian valley filled by marine waters: Fig. 19B) was completely filled by the sediments, the river was raving along its weakly domed alluvial cone (Fig. 19C). Hence, it moved to one of its borders (eastward in this case) where it then cut its new valley (offset with respect to the Messinian one). The cutting of the new valley probably occurred at each momentarily lowering of the global sea-level (such as at 4.9, 3.7 and 3.3 Ma; Miller et al., 2011) before its final acceleration at the earliest Quaternary, when the first Northern

Hemisphere glacials occurred at 2.588 Ma (Fig. 19D; Gibbard et al., 2010). This phenomenon caused the inverted status of the abandonment surface of the Gilbert-type fan deltas (Fig. 8G). Indeed, at Los Molinos de Río Aguas pass, residual conglomerates that we assimilate to topset beds of the Gilbert-type fan deltas constitute a fine residual layer over the gypsum on both sides of the present Río Aguas valley (Figs. 15A and B). These residual fluvial pebbles have been interpreted as Quaternary in age (Harvey and Wells, 1987). This interpretation is however inconsistent with the "aggradation epigenesis" process because these alluvial pebbles, resulting from the sedimentary infilling of the Messinian valley, were deposited a long time before the Quaternary cutting of the modern Río Aguas valley (Fig. 19).

6. Discussion

The Sorbas Basin was at the origin of the two-step scenario of the MSC by Clauzon et al. (1996). It has been, since then, largely accepted by the scientific community (CIESM[2], 2008). However, our study reveals that the MES proposed by Gautier et al. (1994) and Clauzon et al., (1996) was not correctly located in the stratigraphy (MES 1 in Figure 2), because it significantly incises the Yesares gypsums. On the edges of the Sorbas Basin, the MES is at the same stratigraphic place as that proposed by Roveri et al. (2009). However these authors assume continuation of this discontinuity in the central part of the basin (MES 2 in Figure 2) without chronological estimate of the corresponding lack in sedimentation. Evidence of (1) Gilbert-type fan deltas younger than the peak of the MSC (occurrence of *Ceratolithus acutus* in bottomset beds from several places) and (2) the MES near the central part of the Sorbas Basin (Cortijo del Hoyo, Panoramic Viewpoint, Los Molinos de Río Aguas) where it incises

[2] Commisison Internationale pour l'Exploration Scientifique de la Méditerranée.

the Yesares gypsums lead us to conclude that the erosion was subaerial, coeval with the peak of the MSC and thus points out to a stratigraphic gap.

Two cross sections through the basin (location in Figures 3 and 6) derived from our observations and interpretations illustrate the stratigraphic relationships between the units constituting the sedimentary filling of the basin and, more precisely, show their position with respect to the MES or the Messinian Discontinuity (Fig. 16). As a consequence, a new stratigraphic organisation and a precised palaeogeographic evolution of the Sorbas Basin are proposed in a synthetic outline (Fig. 17) that significantly differs from its usual presentation (Fig. 2). Novelties include the following:

- (1) specification of the Messinian Erosional Surface or the Messinian Discontinuity from the edge to the central part of the basin, particularly in several locations above the Yesares gypsums;

- (2) the post-MSC marine reflooding is characterized by the deposition of Gilbert-type fan deltas in the Messinian valleys infilled by marine waters; the Sorbas Member (basinal clays and Sorbas Limestone) is lateral time equivalent of the subaqueous part of the deltas;

- (3) restriction of the concept of the Terminal Carbonate Complex to the reefal carbonates, that is a return to its original definition (Esteban, 1979-1980), the clastic overlying beds added to the TCC by Dabrio and Polo (1995) being in fact the foreset beds of Gilbert-type fan deltas associated with the post-MSC reflooding by marine waters (Fig. 4);

- (4) revised age according to calcareous nannoplankton and planktonic foraminifers of the Sorbas Member deposited after the post-MSC marine reflooding (dated at 5.460 Ma: Bache et al., 2012) and before 5.279 Ma (disappearance of *Triquetrorhabdulus rugosus*; Raffi et al., 2006);

- (5) adjustment to a younger age (i.e. early Zanclean) for the lower part of the entire Zorreras Member which is to be understood as the basinal extension of the topset beds of the Gilbert-type fan deltas;

- (6) updating of the brief return of marine conditions expressed by the bivalve coquina topping the Zorreras loams evidenced by Montenat and Ott d'Estevou (1977) which henceforth does not mark the post-MSC marine reflooding.

During the short duration of the MSC (about 510 kyrs from 5.971 to 5.460 Ma; Bache et al., 2012), the Sorbas Basin recorded the major events relative to sea-level changes including the erosion linked to the peak of the crisis (*ca*. 5.600 – 5.460 Ma; Clauzon et al., 1996; CIESM, 2008; Bache et al., 2012). In an almost continuous regional tectonic context, the imprints of the sea-level changes have been predominantly recorded, making this basin the best place for reconstructing the process of the MSC from onshore archives. Indeed, pollen records from the Alboran Sea (Andalucia G1 and Habibas 1 wells) show that climatic conditions were similarly warm (mean annual temperature estimated between 21 and 23°) and dry (annual precipitations estimated between 400 and 500 mm) for long before and after the peak of the MSC (Fauquette et al., 2006). Using climate modeling, Murphy et al. (2009) concluded to increased moisture on the Atlantic side of Africa between 20 and 30° of North latitude during the peak of the MSC. Wetter conditions have been evidenced in Northwest Africa by geochemical and mineral analyses from ODP Site 659 during the time-interval 5.96 – 5.33 Ma and attributed to a momentarily northward migration of the Inter-Tropical Convergence Zone (Colin et al., 2014). The Bou Regreg (NW Morocco) long pollen record shows a very slight increase in hygrophilous plants from ca. 5.97 to ca. 5.52 Ma (Warny et al., 2003; Fauquette et al., 2006) without any sedimentary change within the clayey succession (Hodell et al., 1994). According to the above-mentioned pollen records, which document relatively stable climatic

conditions in the region, we can consider that climate did not force significantly changes in sedimentation in the Sorbas Basin at the difference of sea-level variations.

Two successive sea-level falls characterize the sedimentary succession in the Sorbas Basin:

- a minor fall occurred at 5.971 Ma, indicated by the gypsum deposition in such an almost completely desiccated peripheral basin and by erosion at the base of the TCC;
- a major fall at *ca*. 5.600 Ma, causing the strong fluvial erosion on land.

Similar stratigraphic relationships between peripheral evaporites (1st step of the MSC) and fluvial erosion (2nd step of the MSC) are known from many outcrops around the Mediterranean Basin, for example (for those that have been published) in Crete (Delrieu et al., 1993), northern Greece (Kavala area: Suc et al., 2009), southern Spain (Bajo Segura Basin: Soria et al., 2005, 2008a and b), and Tunisia (El Euch–El Koundi et al., 2009).

6.1. The sea-level fall at 5.971 Ma and its fluctuations

The amplitude of the sea-level fall at 5.971 Ma may be estimated thanks to observations made in the Sorbas Basin. At Cariatiz (Figs. 3 and 6), the youngest coral reefs prior to the MSC can be considered as representing the coastline just before the MSC (Fig. 16A). These coral reefs (altitude: 500 m) are the closest to the gypsums exposed in the nearby Cruz del Rojo quarry (Figs. 3 and 6) where the uppermost Abad layers reach the altitude of 350 m. It is thus possible to estimate that the water depth in the Sorbas Basin at the beginning of the MSC was about 150 m, a change in sea-level that is in agreement with most of the previous estimates (Dronkert, 1976; Troelstra et al., 1980).

Krijgsman and Meijer (2008) used modelling to refute a global sea-level lowering at the onset of the MSC, concluding that the origin of the crisis was only the result of tectonic uplift in the Gibraltar area. However, the influence of cooling cannot be completely discarded. At Bou Regreg (i.e. the Atlantic outlet of the Rifian Corridor), a dinoflagellate cyst analysis

(Warny and Wrenn, 1997, 2002; Warny et al., 2003) was performed on the same samples that provided a $\delta^{18}O$ record (Hodell et al., 1994), subsequently correlated with that of Site 982 (Hodell et al., 2001). High abundance peaks of *Operculodinium israelianum*, a neritic dinoflagellate cyst, are not only fully consistent with the Antarctic glacials TG 22 and TG 20, but also preceded and followed them (Fig. 18). They indicate that glacio-eustatic variations contributed to water-depth changes in the Rifian Corridor before and after the onset of the MSC (Fig. 18). Shackleton et al. (1995) suggested a 50 m global sea-level fall during Marine Isotope Stages TG 22–20, a value slightly attenuated (30-40 m) by Miller et al. (2011). This global cooling context (ca. 6.10–5.35 Ma: Fig. 18) significantly affected the high latitudes of the North Hemisphere (Larsen et al., 1994). It may have caused, in conjunction with the tectonic narrowing of the Rifian Corridor, the conditions needed for an amplified sea-level fall in the Mediterranean (Vidal et al., 2002; Warny et al., 2003; Drinia et al., 2007; Gargani and Rigollet, 2007), moreover exaggerated in peripheral basins because of the morphology of their difficult connection with the open sea (sill effect). The almost complete desiccation of the Mediterranean peripheral basins may have occurred in such conditions at 5.971 Ma as also evidenced in Sicily (Gautier et al., 1994; Suc et al., 1995; Gargani et al, 2008).

The 150 m sea-level fall probably caused a weak fluvial erosion (Figs. 4 and 16A) nesting the reefal carbonates of the TCC that were deposited during the high sea-level phases as illustrated by the clays of the upper Yesares Member. The corresponding fluctuations are supported by the fossil content of the clayey intercalations within the Yesares gypsums both in the Cruz del Rojo and Peñon Díaz quarries. Sixteen clayey intercalations have been counted by Roveri et al. (2009). The upper clay layers display more marine fossils than the lower ones (Goubert et al., 2001). It suggests that the Yesares Member deposited in a relative transgressive setting (deepening-upward sequence).

As a consequence, we conclude that the Sorbas Basin was almost completely desiccated during each gypsum deposition phase, especially during the eleven lower cycles of Roveri et al. (2009), as supported by the poor malacofauna from the Cuevas de Sorbas.

The basin was partly filled by marine waters as indicated by the intercalated clays of the lower part of the Yesares Member. It was completed when the clay layers of the upper part of the Yesares Member were deposited, allowing correlations with the precession forced global sea-level changes (Krijgsman et al., 2001; Roveri et al., 2009), exaggerated by the sill which probably obstructed the entrance of the basin (Fig. 18).

6.2. Impact of the Mediterranean sea-level drawdown at 5.600 Ma

The major erosion that we observed in the Sorbas Basin affected the Reef Unit and the reefal carbonates of the TCC in the northern part of the basin (Cuesta de Cariatiz, Góchar, Moras; Figs. 7 and 8) and the uppermost beds of the Yesares Member as the most recent eroded levels on the southern margin of the Sorbas Basin (Cortijo del Hoyo, Panoramic Viewpoint; Figs. 9 and 10). This erosion, which affected the youngest gypsums and associated clays, is sealed by sediments with calcareous nannoplankton of Subzone NN12b. It lasted a time-interval from *ca*. 5.600 to *ca*. 5.460 Ma (Bache et al., 2012). It thus corresponds to the fluvial erosion related to the peak of the MSC. The Messinian erosion affected the Sorbas Basin even if its impact was relatively weak in comparison to other peripheral regions such as the Roussillon or the French and Italian Rivieras (Clauzon et al., 1990; Breda et al., 2007, 2009). This difference may be explained by the character of the Sorbas Basin, an inner basin. The magnitude of the fluvial erosion in the Sorbas Basin, taking into account our observations at Cortijo del Hoyo and at the pass close to Los Molinos de Río Aguas is estimated to be about 25–30 m. In these places, the MES is sealed by sediments that we dated from the post-crisis marine reflooding. This implies that the entrenchment of the Messinian valley measured here

is the actual amplitude of fluvial erosion and was not expanded by uplift of the Sorbas area since the MSC, which in addition allowed the exaggerated cutting of the modern valley of the Río Aguas. Figure 3 displays the places where the MES has been observed, the extrapolated potential course of the Messinian valleys within the Sorbas Basin and the outlet from the basin, and also the development areas of two coalescing Gilbert-type fan deltas.

Riding et al. (1998, 1999) and Braga et al. (2006) supported the occurrence of the MES at the base of the Yesares gypsums (MES 3 in Figure 2), following the proposal of Butler et al. (1995) who, in Sicily, placed the MES between the Lower and Upper Evaporites. This location of the MES was disputed by Fortuin et al. (2000) because (1) cyclostratigraphy did not display any gap between the Abad and Yesares members, and (2) the evaporitic formation shows there as in other Mediterranean places a complete record of the gypsum-clay alternations. Soria et al. (2008a, b) evidenced two erosional surfaces in the Bajo Segura Basin (southeast Spain): a weak one at the base of the Messinian gypsums (intra-Messinian unconformity) and a major one at their top (end-Messinian unconformity). Obviously, the latter erosional surface corresponds to the MES in the Sorbas Basin whereas the former one coud be equivalent to the erosion separating the Sorbas reefal carbonates (TCC *s.s.*) from the Reef Unit. The intra-Messinian unconformity of Soria et al. (2008a, b) could also have only a local significance caused by tectonics as it was suggested for the erosional surface separating the Sicilian Lower and Upper Evaporites (Clauzon et al., 1996; El Euch–El Koundi et al., 2009). Indeed, field investigation and cyclostratigraphy done by Roveri et al. (2009) and Manzi et al. (2013) in the Sorbas Basin confirmed that the Yesares Member represents the entire evaporitic series of the peripheral Mediterranean basins and that its correlation with the Sicilian Upper Evaporites was incorrect. We can conclude that the contact of the Yesares gypsums above the Abad deposits does not represent an unconformity in relation with a

significant sea-level drop but at the most a topography resulting from the desiccation of a peripheral basin moulded by gypsums.

As everywhere around the Mediterranean Basin, the almost complete desiccation of the Mediterranean Sea caused fluvial erosion in the Sorbas Basin, which, although it was less intense than in other peripheral basins, is however detectable. The post-MSC sediments are nested within the older deposits except in the central part of the basin where a pseudo-conformity conceals a gap in sedimentation (for example in the Río Aguas section where the Sorbas Limestone conformably overlies the Yesares gypsums – see above: the Messinian Discontinuity; Fig. 16A).

The peak of the MSC did not only change significantly the morphology of the Sorbas Basin but also modified its connection to the Mediterranean Sea, probably with the help of tectonics. Before the MSC, it is generally accepted that the seaward opening of the Sorbas Basin was both to the West and East (Braga et al., 2006; Fortuin and Krijgsman, 2003) while the post-MSC connection was reduced to a narrow ria (i.e. the Messinian valley filled by marine waters) towards the southeast (Fig. 3).

6.3. The Mediterranean reflooding at 5.460 Ma

The process has been subdivided into two steps and dated in Bache et al. (2012). The Sorbas Basin recorded the second brief and huge transgressive phase documented by the coarse debris flow deposits (Fig. 15A–E and 16B) and, immediately after, the prograding Gilbert-type fan deltas (Figs. 7 and 8). In the areas of foreset bed deposition, they correspond to the clastic deposits overlying the TCC *sensu stricto* (Figs. 4, 16A and 18). Topset beds of the Gilbert-type fan deltas, usually almost horizontal, show a dip of about 2–2.5°. This means that the original sedimentary dip of the foreset beds has been somewhat exaggerated (28° to 35°; Figs. 7E and 8F) by the weak tilting of the northern edge of the Sorbas Basin. The possible

"selective" tilting of the clastic deposits topping the TCC *sensu stricto* (i.e. the foreset beds) invoked by some authors (Dabrio and Polo, 1995; Roep et al., 1998; Conesa et al., 1999) must be definitely discarded as it was inconceivable with the prograding advance of the underlying fringing reefs illustrated by an usual dip (Braga and Martín, 1996) similar to that of the clastic foreset beds.

During the deposition of the post-evaporitic units, the palaeogeographical setting of the Sorbas Basin formed a semi-enclosed depression in which were deposited Gilbert-type fan deltas to the North feeding the basin in coarse siliclastics and a lagoonal limestone (Sorbas Limestone) on the western edge of the basin (Ott d'Estevou and Montenat, 1990; Roep et al., 1998; Martín et al., 1999). Both systems evolved basinward to fine-grained siliciclastics (basinal clays) deposited in a slightly deeper depression. The Sorbas Member was deposited during a large transgressive to regressive trend with relatively weak sea-level fluctuations of about 10 to 15 m as evidenced by finning-up parasequences especially in its lower parts (Roep et al., 1998). Its two lower parasequences were deposited in a wedge-shaped accommodation space that we assume being caused by the subaerial erosion during the peak of the MSC. The 25 to 30 m magnitude of suberial erosion cannot only account for the accommodation space necessary to deposit the 60 to 70 m thick series of the Sorbas Member. Such a difference can be solved by the concomitant (1) transgressive trend of the sea level after the reflooding which closed the MSC (Bache et al., 2012) and (2) the ongoing compressive tectonics increasing the flexural trend of the basin (Weijermars et al., 1985).

When the reflooding occurred, seaways followed the Messinian fluvial valleys and momentarily reconnected the Sorbas Basin to the sea. The marine gateway from which the Sorbas Basin was being filled after the peak of the MSC is an important issue. At Los Molinos de Río Aguas, large and disconnected blocks of gypsum are wrapped within a heterogeneous and polymictic matrix (Fig. 15). This particular facies is restricted in a palaeo-

valley morphology and delimits a small area either nested within the gypsum cliff or the underlying Abad Member (Fig. 15B).

According to the new datation of the Zorreras Member, the white chalky layers with a Paratethyan faunal composition most likely correspond to the third Lago Mare event described by Clauzon et al. (2005) as already shown by Do Couto et al. (2014b): high sea-level exchange between the Mediterranean and the Eastern Paratethys at the earliest Zanclean. However, as no dinoflagellate cyst or calcareous nannoplankton were found (these would have indicated influx of surface marine waters), these layers have to be considered as lagoonal episodes just following the Paratethyan water influx (Do Couto et al., 2014b).

Considering the magnetostratigraphic studies by Gautier et al. (1994) and Martín-Suárez et al. (2000), the thin sediments of the Zorreras Hill, i.e. up to and including the coquina, precede the C3An.4n (= Thvera) normal Chron (Fig. 18). As the Zanclean GSSP also precedes this normal chron (Van Couvering et al., 2000), there is no incompatibility to place the entire Zorreras Member into the Zanclean. The mammal fauna described from the lower part of the Zorreras loams has been ascribed to the Turolian mammal age, i.e. “terminal Messinian close to the Mio-Pliocene boundary”, on the basis of the occurrence of four significant species (*Occitanomys alcalai*, *Apodemus* cf. *gorafensis*, *Stephanomys dubari*, *Paraethomys meini*) (Martín-Suárez et al., 2000). However, as indicated by Martín-Suárez et al. (2000), these species have been also recorded in the Ruscinian mammal age, i.e. in the Lower Pliocene (García-Alix et al., 2008). As a consequence, there is no conflicting situation with the mammal fauna if we ascribe the whole Zorreras Member to the Zanclean.

The heterogeneous coarse deposits topping the Zorreras Hill can be continuously followed from the Góchar–Moras and Cariatiz Gilbert-type fan deltas, of which they are the basinal extension. They are widely distributed over the Sorbas Basin. The variety of facies expresses a North-South environmental succession from the alluvial plain (including some small lakes)

to coastal lagoons and finally to the sea. The coquina located in the upper part of the Zorreras Member indicates that the sea was very close to the Zorreras lagoon.

The co-occurrence of *Hirsutella* (*Globorotalia*) *margaritae*, *Ceratolithus acutus* and *Triquetrorhabdulus rugosus* in the clays just overlying the Sorbas Limestone indicates an age comprised between 5.345 and 5.279 Ma for these deposits (Fig. 18). In addition, this calcareous plankton assemblage evidences the entrance of *Hirsutella* (*Globorotalia*) *margaritae* into the Mediterranean Basin significantly before its First Common Occurrence dated at 5.080 Ma (Lourens et al., 2005).

The return of short marine local episodes in the upper part of the continental sedimentary environment, marked by the bivalve coquina of Zorreras and El Cerro Colorado and later by the *Hirsutella* (*Globorotalia*) *margaritae* record at the top-most part of the Gafares section in the nearby Níjar Basin (Bassetti et al., 2006), a layer in which we found, among others, the nannofossil *Ceratolithus acutus*. This indicates an age prior to 5.040 Ma for the younger marine inflow (Fig. 18). According to Bache et al. (2012), the Mediterranean reflooding that followed the MSC occurred at 5.460 Ma, i.e. significantly before the highest Zanclean global sea level (Haq et al., 1987; Miller et al., 2011). Figure 18 summarizes the successive sedimentary layers deposited in the Sorbas Basin between 6.2 and 5.0 Ma with respect to the tectonic evolution of the Gibraltar region and compared to those of the Mediterranean central basins. Reflooding by marine waters was very fast at 5.460 Ma resulting in a sedimentary filling in a Gilbert-type fan delta pattern, which caused the continuous southeastward translation of the coastline. This translation of the shoreline was probably shortly interrupted by high sea-levels (Miller et al., 2011) that caused the momentary returns of marine conditions at about 5.040 Ma (Fig. 18).

7. Conclusion

The Sorbas Basin is a key area for the understanding of the MSC from onshore archives. Our detailed stratigraphic investigation is supported by an unprecedented effort in calcareous nannoplankton and planktonic foraminiferal analyses and supplies new means of accurately dating sediment deposition and erosion in the Sorbas Basin, providing further support for the two-step scenario of the MSC (Clauzon et al., 1996). These new biostratigraphic data show in particular that the Sorbas Member, nested within the Messinian gypsums and in some places overlying them, expresses the marine reflooding which ended the MSC and is mostly of latest Messinian age, maybe of earliest Zanclean age in its uppermost layers (Figs. 17 and 18).

The sense and stratigraphic extension of the TCC have to go back to its original definition. The TCC is to be restricted to the reefal carbonates (= TCC *stricto sensu*) nested within the Reef Unit. The overlying conglomeratic and sandy deposits are the foreset beds of coalescing Gilbert-type fan deltas relative to the marine reflooding of the Mediterranean Basin after the MSC. The bottomset beds of these Gilbert-type fan deltas laterally shift in the basin into different facies (basinal clays and silts in some places, and the coastal Sorbas Limestone) of the Sorbas Member deposited in shallow water conditions, in several places unequivocally nested within the older rocks, particularly those of the Yesares Member.

The MES consists in a well-marked erosional surface, which separates the foreset beds of the Gilbert-type fan deltas from the TCC *sensu stricto* or the Reef Unit on the northern margin of the Sorbas Basin. In the central part of the basin, the Messinian Erosional Surface or locally the Messinian Discontinuity separates the Sorbas Member from the older deposits. It

documents a local down cutting of about 25 to 30 m. At last, the Messinian valley has been fossilized at the pass overhanging Los Molinos de Río Aguas.

The Zorreras Member corresponds to the topset beds of the Gilbert-type fan deltas that are spread over a large area. The abandonment surface of the Gilbert-type fan deltas has been identified at an altitude of about 455 m. It corresponds to the preserved alluvial plain just before the cutting of the modern valley which started during the cooler episodes of the Pliocene and intensified at 2.588 Ma, also well marked by the aggradation epigenesis of the Río Aguas at the gorge of Los Molinos de Río Aguas with respect to its Messinian outlet from the basin.

The Sorbas Lago Mare deposits are earliest Zanclean in age and correspond to the second exchange at high sea level between the Mediterranean and Paratethys evidenced by Clauzon et al. (2005), Popescu et al. (2009), Suc et al. (2011) and Do Couto et al. (2014b). In fact, the three white chalky layers document lagoon environments located just back from the coastal marine ones. The top-most marine influx recorded at the top of the Zorreras Member documents the continuing sea-level rise at the earliest Zanclean (Fig. 18; Bache et al., 2012).

Because of the impact of erosional phase between 5.600 and 5.460 Ma, the methods of cyclostratigraphy and astrochronology appear applicable in the Sorbas Basin to the ante-evaporitic and evaporitic units only. This study should be used as an example for future investigations on the MSC in the peripheral Mediterranean basins.

Acknowledgements

This paper is the last study leadered by Georges Clauzon who died during its achievement. It is also dedicated to the memory of the late François Gautier who was the first to conduct a

calibration of the Messinian Salinity Crisis based on magnetostratigraphy particularly from the Sorbas Basin. His pioneering and precise work was not recognized as it should have been. For some of us, the beginning of this investigation has been funded by previous CNRS projects (RCP 826, Programme ECLIPSE), the recent field research has been supported by the Projects AMEDITER ("Actions Marges" CNRS/INSU Programme), "Bassins néogènes et manteau en Méditerranée" (TerMEx CNRS/INSU Programme), the CIFRE PhD grant N° 584/2010 (TOTAL/UPMC) and the Research Project CGL2010-15047 (Spanish Government). These programs have allowed several common trips to the Sorbas Basin, which permitted intense discussions between the co-authors and the resulting large collaboration that formed the basis of this paper.

Dr. José-Maria Calaforra is thanked for guiding one of us (L.M.) in the Sorbas area and for the fruitful discussion on this occasion. José Clavero Casto and José Antonio Acha Jiménez, successive Directors of the Cruz del Rojo quarry (Explotaciones Rio de Aguas, KOMPASS Almería Gypsum Society) and Diego Contreras, Director of the Cuevas de Sorbas, offered many facilities for entering the territory under their respective responsibility. F.J. Sierro is acknowledged for providing unpublished information and examining foraminifers from some of our preliminary samples. We particularly express gratitude to the scientists who reviewed this manuscript and, by their constructive comments and suggestions, helped us to improve it.

References

Aufgebauer, A., McCann, T., 2010. Messinian to Pliocene transition in the deep part of the Sorbas Basin, SE Spain – a new description of the depositional environment during the Messinian Salinity Crisis. N. Jb. Geol. Paläont. 259(2), 177–195.

Augier, R., Jolivet, L., Robin, C., 2005. Late orogenic doming in the eastern Betic Cordilleras: final exhumation of the Nevado-Filabride complex and its relation to basin genesis. Tectonics 24, TC4003, doi: 10.1029/2004TC001687.

Bache, F., Popescu, S.-M., Rabineau, M., Gorini, C., Suc, J.-P., Clauzon, G., Olivet, J.-L., Rubino, J.-L., Melinte-Dobrinescu, M.C., Estrada, F., Londeix, L., Armijo, R., Meyer, B., Jolivet, L., Jouannic, G., Leroux, E., Aslanian, D., Batzan, J., Dos Reis, A.T., Mocochain, L., Dumurdžanov, N., Zagorchev, I., Lesić, V., Tomić, D., Çağatay, M.N., Brun, J.-P., Sokoutis, D., Csato, I., Ucarkus, G., Çakir, Z., 2012. A two-step process for the reflooding of the Mediterranean after the Messinian Salinity Crisis. Bas. Res. 24, 125–153.

Bassetti, M.A., Miculan, P., Sierro, F.J., 2006. Evolution of depositional environments after the end of Messinian Salinity Crisis in Nijar basin (SE Betic Cordillera). Sed. Geol. 188–189, 279–295.

Berggren, W.A., Kent, D.V., Swisher III, C.C., Aubry, M.-P., 1995. A revised Cenozoic geochronology and chronostratigraphy. In: Berggren, W.A., Kent, D.V., Aubry, M.-P.,. Hardenbol, J (Eds.), Geochronology, Time Scales and Global Stratigraphic Correlation: A Unified Temporal Framework for an Historical Geology. Spec. Publ., Soc. Econ. Paleontol. Mineral. 54, 141–212.

Bolli, H.M., 1966. The Planktonic Foraminifera in Well Bodjonegoro-1 of Java. Eclogae Geol. Helv. 59(1), 449–465.

Bourillot, R., Vennin, E., Rouchy, J.-M., Blanc-Valleron, M.-M., Caruso, A., Durlet, C., 2010a. The end of the Messinian Salinity Crisis in the western Mediterranean: Insights from the carbonate platforms of south-eastern Spain. Sedim. Geol. 229, 224–253.

Bourillot, R., Vennin, E., Rouchy, J.-M., Durlet, C., Rommevaux, V., Kolodka, C., Knap, F., 2010b. Structure and evolution of a Messinian mixed carbonate-siliclastic platform: the role of evaporites (Sorbas Basin, South-east Spain). Sedimentology 57, 477–512.

Braga, J.C., Martín, J.M., 1996. Geometries of reef advance in response to relative sea-level changes in a Messinian (uppermost Miocene) fringing reef (Cariatiz reef, Sorbas Basin, SE Spain). Sedim. Geol. 107, 61–81.

Braga, J.C., Martín, J.M., Riding, R., Aguirre, J., Sánchez-Almazo, I., Dinarès-Turell, J. (2006) Testing models for the Messinian salinity crisis: The Messinian record in Almería, SE Spain. Sedim. Geol. 188–189, 131–154.

Breda, A., Mellere, D., Massari, F., 2007. Facies and processes in a Gilbert-delta-filled incised valley (Pliocene of Ventimiglia, NW Italy). Sedim. Geol. 200, 31–55.

Breda, A., Mellere, D., Massari, F., Asioli, A., 2009. Vertically stacked Gilbert-type fan deltas of Ventimiglia (NW Italy): The Pliocene record pf an overfilled Messinian incised valley. Sedim. Geol. 219, 58–76.

Butler, R.W.H., Lickorish, W.H., Grasso, M.M., Pedley, H.M., Ramberti, L., 1995. Tectonics and sequence stratigraphy in Messinian basins, Sicily: constraints on the initiation and termination of the Mediterranean salinity crisis. Geol. Soc. Am. Bull. 107, 425–439.

Calaforra, J.M., Pulido-Bosch, A., 2003. Evolution of the gypsum karst of Sorbas (SE Spain). Geomorphology 50, 173–180.

Carbonnel, G., 1978. La zone à *Loxoconcha djaffarovi* Schneider (Ostracoda, Miocène supérieur) ou le Messinien de la vallée du Rhône. Rev. Micropaléontol. 21, 106–118.

CIESM (Antón, J., Çağatay, M.N., De Lange, G., Flecker, R., Gaullier, V., Gunde-Cimerman, N., Hübscher, C., Krijgsman, W., Lambregts, P., Lofi, J., Lugli, S., Manzi, V., McGenity, T.J., Roveri, M., Sierro, F.J. , Suc J.-P., 2008. Executive Summary. In: Briand, F. (Ed.), The Messinian Salinity Crisis from mega-deposits to microbiology – A consensus report, CIESM Workshop Monographs 33, 7–28.

Cita, M.B., Colombo, L., 1979. Sedimentation in the latest Messinian at Capo Rossello (Sicily). Sedimentology 26, 497–522.

Cita, M.B., Vismara Schilling, A., Bossio, A., 1980. Stratigraphy and paleoenvironment of the Cuevas de Almanzora section (Vera Basin), a reinterpretation. Riv. Ital. Paleontol. 86(1), 215–240.

Civis, J., Martinell, J., De Porta, J., 1979. Presencia de *Cyprideis pannonica pseudoagrigentina* DECIMA en el Miembro Zorreras (Sorbas, Almería). Studia Geol. 15, 57–62.

Clauzon, G., 1980. Révision de l'interprétation géodynamique du passage miocène-pliocène dans le basin de Vera (Espagne méridionale): les coupes d'Antas et de Cuevas del Almanzora. Riv. Ital. Paleontol. 86(1), 203–214.

Clauzon, G., 1990. Restitution de l'évolution géodynamique néogène du bassin du Roussillon et de l'unité adjacente des Corbières d'après les données écostratigraphiques et paléogéographiques. Paléobiol. Cont. 17, 125–155.

Clauzon, G., 1996. Limites de séquences et évolution géodynamique. Géomorphologie 1, 3–22.

Clauzon, G., Suc, J.-P., Aguilar, J.-P., Ambert, P., Cappetta, H., Cravatte, J., Drivaliari, A., Doménech, R., Dubar, M., Leroy, S., Martinell, J., Michaux, J., Roiron, P., Rubino, J.-L., Savoye, B., Vernet, J.-L., 1990. Pliocene geodynamic and climatic evolutions in the French Mediterranean region. Paleontol. Evoluc. Spec. Mem. 2, 132–186.

Clauzon, G., Suc, J.-P., Gautier, F., Berger, A., Loutre, M.-F., 1996. Alternate interpretation of the Messinian salinity crisis: Controversy resolved? Geology 24, 363–366.

Clauzon, G., Suc, J.-P., Popescu, S.-M., Marunțeanu, M., Rubino, J.-L., Marinescu, F., Melinte, M.C., 2005. Influence of the Mediterranean sea-level changes over the Dacic Basin (Eastern Paratethys) in the Late Neogene. The Mediterranean Lago Mare facies deciphered. Bas. Res. 17, 437–462.

Clauzon, G., Suc, J.-P., Melinte-Dobrinescu, M.C., Jouannic, G., Jolivet, L., Rubino, J.-L., Popescu, S.-M., Gorini, C., Bache, F., Estrada, F., 2009. New insights from the Andalusian Sorbas and Vera basins. 13rd RCMNS Congress, Naples, Acta Naturalia de L'Ateneo Parmense 45(1/4), 334–335.

Clauzon, G., Suc, J.-P., Popescu, S.-M., Melinte-Dobrinescu, M.C., Quillévéré, F., Warny, S., Fauquette, S., Armijo, R., Meyer, B., Rubino, J.-L., Lericolais, G., Gillet, H., Çağatay, N., Ucarkus, G., Escarguel, G., Jouannic, G., Dalesme, F., 2008. Chronology of the Messinian events and paleogeography of the Mediterranean region *s.l.* CIESM Workshop Monographs 33, 31–37.

Colalongo, M.L. (1968) Ostracodi del neostratotipo del Messiniani. Giorn. Geol. 35(2), ser. 2, 67–72.

Colin, C., Siani, G., Liu, Z., Blamart, D., Skonieczny, C., Zhao, Y., Bory, A., Frank, N., Duchamp-Alphonse, S., Thil, F., Richter, T., Kissel, C., Gargani, J., 2014. Late Miocene to early Pliocene climate variability off NW Africa (ODP Site 659). Palaeogeogr., Palaeoclimatol., Palaeoecol. 401, 81–95.

Conesa, G., 1997. Géométrie et biosédimentologie d'une plate-forme carbonate messinienne (basin de Sorbas, sud-est de l'Espagne) (PhD Thesis). University of Provence, Marseilles, p. 269.

Conesa, G., Saint Martin, J.-P., Cornée, J.-J., Muller, J., 1999. Nouvelles contraintes sur la crise de salinité messinienne par l'étude d'une plate-forme carbonatée (bassin de Sorbasn Espagne). C. R. Acad. Sci. Paris Earth Planet. Sci. 328, 81–87.

Cornée, J.-J., Saint Martin, J.-P., Conesa, G., Münch, P., André, J.-P., Saint Martin, S., Roger, S., 2004. Correlations and sequence stratigraphic model for Messinian carbonate platforms of the western and central Mediterranean. Int. J. Earth Sci. 93, 621–633.

Cuevas Castell, J.M., Betzler, C., Rössler, J., Hüssner, H., Peinl, M., 2007. Integrating outcrop data and forward computer modelling to unravel the development of a Messinian carbonate platform in SE Spain (Sorbas Basin). Sedimentology 54, 423–441.

Dabrio, C.J., Polo, M.D., 1995. Oscilaciones eustáticas de alta frequencia en el Neógeno superior de Sorbas (Almería, sureste de España). Geogaceta 18, 75–78.

Decima, A., 1964. Ostracodi del Gen. *Cyprideis* Jones del Neogene e del Quaternario italiani. Paleontol. Ital. 57, 81–133.

Delrieu, B., Rouchy, J.-M., Foucault, A., 1993. La surface d'érosion finimessinienne en crète centrale (Grèce) et sur le pourtour méditerranéen: Rapports avec la crise de salinité méditerranéenne. C. R. Acad. Sci. Paris 2 Ser. 2 316, 527–533.

Do Couto, D., Gumiaux, C., Augier, R., Lebret, N., Folcher, N., Jouannic, G., Jolivet, L., Suc, J.-P., Gorini, C., 2014a. Tectonic inversion of an asymmetric graben: Insights from a combined field and gravity survey in the Sorbas basin. Tectonics 33(7), 1360–1383.

Do Couto, D., Popescu, S.-M., Suc, J.-P., Melinte-Dobrinescu, M.C., Barhoun, N., Gorini, C., Jolivet, L., Poort, J., Jouannic, G., Auxietre, J.-L., 2014b. Lago Mare and the Messinian Salinity Crisis: Evidences from the Alboran Sea (S. Spain). Mar. Petrol. Geol. 52, 57–76.

Drinia, H., Antonarakou, A., Tsaparas, N., Kontakiotis, G., 2007. Palaeoenvironmental conditions preceding the Messinian Salinity Crisis: A case study from Gavdos Island. Geobios 40, 251–265.

Dronkert, H., 1976. Late Miocene evaporites in the Sorbas Basin and adjoining areas. Mem. Soc. Geol. Ital. 16, 341–361.

Dronkert, H., 1977. The evaporites of the Sorbas basin. Rev. Inst. Invest. Geol. Dip. Provincial Univ. Barcelona 32, 55–76.

El Euch–El Koundi, N., Ferry, S., Suc, J.-P., Clauzon, G., Melinte-Dobrinescu, M.C., Gorini, C., Safra, A., El Koundi, M., Zargouni, F., 2009. Messinian deposits and erosion in

northern Tunisia: Inferences on the Sicily Strait during the Messinian Salinity Crisis. Terra Nova 21, 41–48.

Esteban, M., 1979–1980. Significance of the Upper Miocene Reefs in the Western Mediterranean. Palaeogeogr. Palaeoclimatol. Palaeoecol. 29, 169–188.

Esteban, M., Giner, J., 1980. Messinian coral reefs and erosion surfaces in Cabo de Gata (Almeria, SE Spain). Acta Geol. Hisp. 15(4), 97–104.

Fauquette, S., Suc, J.-P., Bertini, A., Popescu, S.-M., Warny, S., Bachiri Taoufiq, N., Perez Villa, M.-J., Chikhi, H., Subally, D., Feddi, N., Clauzon, G., Ferrier, J., 2006. How much did climate force the Messinian salinity crisis? Quantified climatic conditions from pollen records in the Mediterranean region. Palaeogeogr., Palaeoclimatol., Palaeoecol. 238(1-4), 281–301.

Fortuin, A.R., Krijgsman, W., 2003. The Messinian of the Nijar Basin (SE Spain): sedimentation, depositional environments and paleogeographic evolution. Sediment. Geol. 160, 213–242.

Fortuin, A.R., Krijgsman, W., Hilgen, F.J., Sierro, F.J., 2000. Late Miocene Mediterranean desiccation: topography and significance of the ‘Salinity Crisis’ erosion surface on-land in southeast Spain: Comment. Sediment. Geol. 133, 167–174.

Garcia-Castellanos, D., Villaseñor, A., 2011. Messinian salinity crisis regulated by competing tectonics and erosion at the Gibraltar arc. Nature 480, 359–363.

García-Alix, A., Minwer-Barakat, R., Martín, J.M., Martín Suárez, E., Freudenthal, M., 2008. Biostratigraphy and sedimentary evolution of Late Miocene and Pliocene continental deposits of the Granada Basin (southern Spain). Lethaia 41, 431–446.

García-Dueñas, V., Balanyá, J.C., Martínez-Martínez, J.M., 1992. Miocene extensional detachments in the outcropping basement of the Northern Alboran Basin (Betics) and their tectonic implications. Geo-Marine Lett. 12, 88–95.

Gargani, J., Moretti, I., Letouzey, J., 2008. Evaporite accumulation during the Messinian Salinity Crisis: The Suez Rift case. Geophys. Res. Lett. 35, L02401, doi:10.1029/2007GL032494, 6 p.

Gargani, J., Rigollet, C., 2007. Mediterranean Sea level variations during the Messinian salinity crisis. Geophys. Res. Lett. 34, L10405, doi:10.1029/2007GL029885, 5 p.

Gaudant, J., Ott d'Estevou, P., 1985. Première découverte d'*Aphanius crassicaudus* (Agassiz) (poisson téléostéen, Cyprinodontidae) dans le Messinien post-évaporitique d'Andalousie. Estudios Geol. 41, 93–98.

Gautier, F., Clauzon, G., Suc, J.-P., Cravatte, J., Violanti, D., 1994. Age et durée de la crise de salinité messinienne. C.-R. Acad. Sci. Paris Ser. 2 318, 1103–1109.

Gibbard, P., Head, M.J., Walker, M. and the other members of the International Subcommission on Quaternary Stratigraphy (Alloway, B., Beu, A.G., Coltorti, M., Hall, V.M., Jiaqi, L., Knudsen, K.L., van Kolfschoten, T., Litt, T., Marks, L., McManus, J., Partridge, T.C., Piotrowski, J.A., Pillans, B., Rousseau, D.-D., Suc, J.-P., Tesakov, A.S., Turner, C., Zazo, C.), 2010. Formal ratification of the Quaternary System/Period and the Pleistocene Series/Epoch with a base at 2.58 Ma. Journ. Quat. Sci. 25(2), 96–102.

Gliozzi, E., Ceci, M.E., Grossi, F., Ligios, S., 2007. Paratethyan Ostracod immigrants in Italy during the Late Miocene. Geobios 40, 325–337.

Gliozzi, E., Grossi, F., Cosentino, D., 2006. Late Messinian biozonation in the Mediterranean area using Ostracods: a proposal. In: Roveri, M. (Ed.), The Messinian salinity crisis revisited-II, Acta naturalia de "L'Ateneo Parmense", abstract A.21SS.3.

Goubert, E., Néraudeau, D., Rouchy, J.M., Lacour, D., 2001. Foraminiferal record of environmental changes: Messinian of the Los Yesos area (Sorbas Basin, SE Spain). Palaeogeogr. Palaeoclimatol. Palaeoecol. 175, 61–78.

Haq, B.U., Hardenbol, J., Vail, P.R., 1987. Chronology of fluctuating sea levels since the Triassic (250 million years ago to present). Science 235, 1156–1167.

Harvey, A.M., Wells, S.G., 1987. Response of Quaternary fluvial systems to differential epeirogenic uplift: Aguas and Feos river systems, southeast Spain. Geology 15, 689–693.

Hodell, D.A., Benson, H.B., Kent, D.V., Boersma, A., Rakic-El Bied, K., 1994. Magnetostratigaphic, biostratigraphic, and stable isotope stratigraphy of an Upper Miocene drill core from the Salé Briqueterie (northwestern Morocco): A high-resolution chronology for the Messinian stage. Paleoceanography 9, 835–855.

Hodell, D.A., Curtis, J.H., Sierro, F.J., Raymo, M.E. (2001) Correlation of late Miocene to early Pliocene sequences between the Mediterranean and North Atlantic. Paleoceanography 16, 164–178.

Hsü, K.J., Cita, M.B., Ryan, W.B.F., 1973a. The origin of the Mediterranean evaporites, in: Ryan, W.B.F., Hsü, K.J., al. (Eds.), Initial Reports of Deep Sea Drilling Project. U.S. Government Printing Office, Washington, pp. 1203-1231.

Johnson, C., Harbury, N., Hurford, A.J., 1997. The role of extension in the Miocene denudation of the Nevado–Filabrides Complex, Betic Cordillera (SE Spain). Tectonics 16, 189–204.

Jolivet, L., Augier, R., Robin, C., Suc, J.-P., Rouchy, J.M., 2006. Lithospheric-scale geodynamic context of the Messinian salinity crisis. Sediment. Geol. 188–189, 9–33.

Kennett, J.P., Srinivasan, M.S., 1983. Neogene planktonic foraminifera: a phylogenetic atlas. Hutchinson and Ross Publishing Company, Stroudsburg, Pennsylvania, 265 pp.

Krijgsman, W., Fortuin, A.R., Hilgen, F.J., Sierro, F.J., 2001. Astrochronology for the Messinian Sorbas basin (SE Spain) and orbital (precessional) forcing for evaporite cyclicity. Sediment. Geol. 140, 43–60.

Krijgsman, W., Gaboardi, S., Hilgen, F.J., Iaccarino, S., de Kaenel, E., van der Laan, E., 2004. Revised astrochronology for the Ain el Beida section (Atlantic Morocco): No glacio-eustatic control for the onset of the Messinian Salinity Crisis. Stratigraphy 1, 87–101.

Krijgsman, W., Hilgen, F.J., Raffi, I., Sierro, F.J., Wilson, D.S., 1999. Chronology, causes and progression of the Messinian salinity crisis. Nature 400, 652–655.

Krijgsman, W., Meijer, P.Th., 2008. Depositional environments of the Mediterranean "Lower Evaporites" of the Messinian salinity crisis: Constraints from quantitative analyses. Mar. Geol. 253, 72–81.

Lacour, D., Néraudeau, D., 2000. Evolution de la diversité des *Brissopsis* (Echinoida, Spatangoida) en Méditerranée depuis la "crise messinienne": application paléoécologique aux *B. lyrifera* intragypses de Sorbas (SE Espagne). Geodiversitas 22, 509–523.

Lacour, D., Lauriat-Rage, A., Saint Martin, J.-P., Videt, B., Néraudeau, D., Goubert, E., Bongrain, M., 2002. Les associations de bivalves (Mollusca, Bivalvia) du Messinien du bassin de Sorbas (SE Espagne). Geodiversitas 24, 641–657.

Landau, B., La Perna, R., Marquet, R., 2006. The Early Pliocene gastropoda (Mollusca) of Estepona, Southern Spain. Part 6: Triphoroidea, Epitonioidea, Eulimoidea. Palaeontos 10, 1–96.

Larsen, H.C., Saunders, A.D., Clift, P.D., Beget, J., Wei, W., Spezzaferri, S. and ODP Leg 152 Scientific Party, 1994. Seven Million Years of Glaciation in Greenland. Science 264, 952–955.

Lourens, L.J., Hilgen, F.J., Laskar, J., Shackleton, N.J., Wilson, D., 2005. The Neogene period. In: Gradstein, F.M., Ogg, J.G., Smith, A.G. (Eds.), A geological Time Scale 2004, Cambridge University Press, pp. 409–440.

Manzi, V., Gennari, R., Hilgen, F., Krijgsman, W., Lugli, S., Roveri, M., Sierro, F.J., 2013. Age refinement of the Messinian salinity crisis onset in the Mediterranean. Terra Nova 25, 315–322.

Martín, J.M., Braga, J.C., 1994. Messinian events in the Sorbas Basin in southeastern Spain and their implications in the recent history of the Mediterranean. Sedim. Geol. 90, 257–268.

Martín, J.M., Braga, J.C., Sánchez-Almazo, I.M., 1999. The Messinian record of the outcropping marginal Alboran basin deposits: significance and implications, In: Zahn, R., Comas, M.C., Klaus A. (Eds.), Proceedings of the Ocean Drilling Program, Scientific Results, vol. 161, pp. 543–551.

Martín-Suárez, E., Freudenthal, M., Krijgsman, W., Rutger Fortuin, A., 2000. On the age of the continental deposits of the Zorreras Member (Sorbas Basin, SE Spain). Geobios 33, 505–512.

Martínez-Martínez, J.M., Soto, J.I., Balanyá, J.C., 2002. Orthogonal folding of extensional detachments: structure and origin of the Sierra Nevada elongated dome (Betics, SE Spain). Tectonics 21(3), 1012, doi:10.1029/2001TC001283.

Martini, E., 1971. Standard Tertiary and Quaternary calcareous nannoplankton zonation. In: Farinacci, A. (Ed.), Proceedings of the Second International Conference on Planktonic Microfossils Roma, Ed. Tecnoscienza, Rome, 2, pp. 739–785.

Melinte-Dobrinescu, M.C., Suc, J.-P., Clauzon, G., Popescu, S.-M., Armijo, R., Meyer, B., Biltekin, D., Çağatay, M.N., Ucarkus, G., Jouannic, G., Fauquette, S., Çakir, Z., 2009. The Messinian Salinity Crisis in the Dardanelles region: Chronostratigraphic constraints. Palaeogeogr. Palaeoclimatol. Palaeoecol. 278, 24–39.

Michalzik, D., 1996. Lithofacies, diagenetic spectra and sedimentary cycles of Messinian (Late Miocene) evaporites in SE Spain. Sediment. Geol. 106, 203–222.

Miller, K.G., Mountain, G.S., Wright, J.D., Browning, J.V., 2011. A 180-million-year record of sea level and ice volume cariations from continental margin and deep-sea isotopic records. Oceanography 24(2), 40–53.

Montenat, C., Ott d'Estevou, P., 1977. Présence du Pliocène marin dans le basin de Sorbas (Espagne méridionale). Conséquences paléogéographiques et tectoniques. C. R. somm. Soc. Géol. France 4, 209–211.

Montenat, C., Ott d'Estevou, P., Plaziat, J.-C., Chapel, J., 1980. La signification des faunes marines contemporaines des évaporites messiniennes dans le Sud-Est de l'Espagne. Conséquences pour l'interprétation des conditions d'isolement de la Méditerranée occidentale. Géol. Médit. 7(1), 81–90.

Murphy, L.N., Kirk-Davidoff, D.B., Mahowald, N., Otto-Bl, B.L., 2009. A numerical study of the climate response to lowered Mediterranean Sea level during the Messinian Salinity Crisis. Palaeogeogr., Palaeoclimatol., Palaeoecol. 279, 41–59.

Néraudeau, D., Videt, B., Courville, P., Goubert, E., Rouchy, J.-M., 2002. Corrélation des niveaux fossilifères marins interstratifiés dans les gypses messiniens, entre la carrière de Los Yesos et la carrière de Molinos de Aguas (bassin de Sorbas, SE Espagne). Geodiversitas 24, 659–667.

Orszag-Sperber, F., 2006. Changing perspectives in the concept of "Lago Mare" in Mediterranean late Miocene evolution. Sedim. Geol. 188–189, 259–277.

Ott d'Estevou, P. (coordinator), 1990. Almeria–Sorbas. Documents et travaux IGAL, Geologicap map, 1.

Ott d'Estevou, P., Montenat, C., 1990. Le bassin de Sorbas – Tabernas. Documents et travaux IGAL 12–13, 101–128.

Perch-Nielsen, K., 1985. Cenozoic calcareous nannofossils. In: Bolli, H.M. Saunders, J.B., Perch-Nielsen, K. (Eds.), Plankton Stratigraphy, Cambridge University Press, p. 427–554.

Poppe, G.T., Goto, Y., 1993. European Seashells, Verlag Christa Hemmen, vol. II, 221 pp.

Popescu, S.-M., Dalesme, F., Jouannic, G., Escarguel, G., Head, M.J., Melinte-Dobrinescu, M.C., Sütő-Szentai, M., Bakrac, K., Clauzon, G., Suc, J.-P., 2009. *Galeacysta etrusca* complex, dinoflagellate cyst marker of Paratethyan influxes into the Mediterranean Sea before and after the peak of the Messinian Salinity Crisis. Palynology 33(2), 105–134.

Raffi, I., Backman, J., Fornaciari, E., Pälike, H., Rio, D., Lourens, L.J., Hilgen, F.J., 2006. A review of calcareous nannofossil astrobiochronology encompassing the past 25 million years. Quat. Sci. Rev. 25, 3113–3137.

Riding, R., Braga, J.C., Martín, J.M., Sánchez-Almazo, I., 1998. Mediterranean Messinian Salinity Crisis: constraints from a coeval marginal basin, Sorbas, southeastern Spain. Mar. Geol. 146, 1–20.

Riding, R., Braga, J.C., Martín, J.M., 1999. Late Miocene Mediterranean desiccation: topography and significance of the ‘Salinity Crisis’ erosion surface on-land in southeast Spain. Sediment. Geol. 123, 1–7.

Riding, R., Braga, J.C., Martín, J.M., 2000. Late Miocene Mediterranean desiccation: topography and significance of the `Salinity Crisis' erosion surface on-land in southeast Spain: Reply. Sediment. Geol. 133, 175–184.

Roep, Th.B., Dabrio, C.J., Fortuin, A.R., Polo, M.D., 1998. Late highstand patterns of shifting and stepping coastal barriers and washover-fans (late Messinian, Sorbas Basin, SE Spain). Sediment. Geol. 116, 27–56.

Roep, Th.B., Van Harten, D., 1978. Sedimentological and ostracodological observations on Messinian post-evaporite deposits of some southeastern Spanish basins. Ann. Géol. Pays Hellén. Spec. Mem. 3, 1037–1044.

Rouchy, J.-M., 1976. Sur la genèse de deux principaux types de gypse (finement lité et en chevrons) du Miocène terminal de Sicile et d'Espagne méridionale. Rev. Géogr. Phys. Géol. Dyn. 18(4), ser. 2, 347–364.

Roveri, M., Gennari, R., Lugli, S., Manzi, V., 2009. The Terminal Carbonate Complex: the record of sea-level changes during the Messinian salinity crisis. GeoActa 8, 63–77.

Ruegg, G.J.H., 1964. Geologische onderzoekingen in het bekken van Sorbas. Intern. Rep. Geol. Inst. Univ. of Amsterdam, p. 67.

Saint-Martin, J.-P., Néraudeau, D., Lauriat-Rage, A., Goubert, E., Secrétan, S., Babinot, J.-F., Boukli-Hacene, S., Pouyet, S., Lacour, D., Pestrea, S., Conesa, G., 2000. La faune interstratifiée dans les gypses messiniens de Los Yesos (bassin de Sorbas, SE Espagne): Implications. Geobios 33, 637–649.

Sánchez-Almazo, I.M., 1999. Evolución paleoambiental de las cuencas neógenas de Almería en el Messiniense (PhD Thesis). Univ. of Granada, 270 p.

Sánchez-Almazo, I.M., Bellas, S.M., Civis, J., Aguirre, J., 1999. Palaeoenvironmental and biostratigraphical significance oft he microfossil assemblages of the uppermost Messinian marine deposits oft he Sorbas Basin (Almería, SE Spain). Workshop oft he Eropean Palaeontological Association, Lisbon, Abstracts, 102–106.

Sánchez-Almazo, I.M., Braga, J.C., Dinarès-Turell, J., Martín, J.M., Spiro, B., 2007. Palaeoceanographic controls on reef deposition: the Messinian Cariatiz reef (Sorbas Basin, Almería, SE Spain). Sedimentology 54, 637–660.

Sanz de Galdeano, C., Vera, J.A., 1992. Stratigraphic record and paleogeographical context of the Neogene basins in the Betic Cordillera, Spain. Bas. Res. 4, 21–36.

Serpelloni, E., Vannucci, G., Pondrelli, S., Argnani, A., Casula, G., Anzidei, M., Baldi, P., Gasperini, P., 2007. Kinematics of the Western Africa-Eurasia plate boundary from focal mechanisms and GPS data. Geophys. J. Int. 169, 1180–1200.

Shackleton, N.J., Hall, M.A., Pate, D., 1995. Pliocene stable isotope stratigraphy of Site 846. In: Pisias, N.G., Mayer, L.A., Janecek, T.R. Palmer-Julson, A., van Andel, T.H. (Eds.), Proceedings of the Ocean Drilling Program, Scientific Results, vol. 138, U.S. Gov. Print. Off., Washington, p. 337–355.

Sierro, F.J., Flores, J.A., Zamarreño, I., Vázquez, A., Utrilla, R., Francès, G., Hilgen, F.J., Krijgsman, W., 1999. Messinian pre-evaporite sapropels and precession-induced oscillations in western Mediterranean climate. Mar. Geol. 153, 137–146.

Sierro, F.J., Hilgen, F.J., Krijgsman, W., Flores, J.A., 2001. The Abad composite (SE Spain): a Messinian reference section for the Mediterranean and the APTS. Palaeogeogr. Palaeoclimatol. Palaeoecol. 168, 141–169.

Soria, J.M., Caracuel, J.E., Corbí, H., Dinarès-Turell, J., Lancis, C., Tent-Manclús, J.E., Viseras, C., Yébenes, A., 2008a. The Messinian–early Pliocene stratigraphic record in the southern Bajo Segura Basin (Betic Cordillera, Spain): Implications for the Mediterranean salinity crisis. Sediment. Geol. 203, 267–288.

Soria, J.M., Caracuel, J.E., Corbí, H., Dinarès-Turell, J., Lancis, C., Tent-Manclús, J.E., Yébenes, A., 2008b. The Bajo Segura Basin (SE Spain): implications for the Messinian salinity crisis in the Mediterranean margins. Stratigraphy 5(3–4), 257–263.

Soria, J.M., Caracuel, J.E., Yébenes, A., Fernández, J., Viseras, C., 2005. The stratigraphic record of the Messinian salinity crisis in the northern margin of the Bajo Segura Basin (SE Spain). Sediment. Geol. 179, 225–247.

Suc, J.-P., Clauzon, G., Armijo, R., Meyer, B., Melinte-Dobrinescu, M.C., Popescu, S.-M., Lericolais, G., Gillet, H., Çağatay, M.N., Jouannic, G., Brun, J.-P., Sokoutis, D., Ucarkus, G., Çakir, Z., 2009. The Messinian Salinity Crisis in the Northeastern Aegean – Black Sea region. 13rd RCMNS Congress Naples, Acta Naturalia de L'Ateneo Parmense 45(1–4), 116–117.

Suc, J.-P., Do Couto, D., Melinte-Dobrinescu, M.C., Macaleț, R., Quillévéré, F., Clauzon, G., Csato, I., Rubino, J.-L., Popescu, S.-M., 2011. The Messinian Salinity Crisis in the dacic basin (SW Romania) and early Zanclean Mediterranean – Paratethys high sea-level connection. Palaeogeogr., Palaeoclimatol., Palaeoecol. 310, 256–272.

Suc, J.-P., Violanti, D., Londeix, L., Poumot, C., Robert, C., Clauzon, G., Turon, J.-L., Ferrier, J., Chikhi, H., Cambon, G., Gautier, F., 1995. Evolution of the Messinian Mediterranean environments: the Tripoli Formation at Capodarso (Sicily, Italy). Rev. Palaeobot. Palynol. 87, 51–79.

Troelstra, S.R., van de Poel, H.M., Huisman, C.H.A., Geerlings, L.P.A., Dronkert, H., 1980. Paleoecological changes in the latest Miocene of the Sorbas Basin, SE Spain. Géol. Médit. 7, 115–126.

Van Couvering, J.A., Castradori, D., Cita, M.B., Hilgen, F.J., Rio, D., 2000. The base of the Zanclean Stage and of the Pliocene Series. Episodes 23(3), 179–187.

Vidal, L., Bickert, T., Wefer, G., Röhl, U., 2002. Late Miocene stable isotope stratigraphy of SE Atlantic ODP Site 1085: Relation to Messinian events. Mar. Geol. 180, 71–85.

Vissers, R.L. M., Platt, J.P., Van der Wal, D., 1995. Late orogenic extension of the Betic Cordillera and the Alboran Domain: A lithospheric view. Tectonics 14, 786–803.

Warny, S., Bart, P.J., Suc, J.-P., 2003. Timing and progression of climatic, tectonic and glacioeustatic influences on the Messinian Salinity Crisis. Palaeogeogr., Palaeoclimatol., Palaeoecol. 202, 59–66.

Warny, S., Wrenn, J.H., 1997. New species of Dinoflagellate cysts from the Miocene-Pliocene boundary on the Atlantic coast of Morocco. Rev. Palaeobot. Palynol. 96, 281–304.

Warny, S., Wrenn, J.H., 2002. Upper Neogene dinoflagellate cyst ecostratigraphy of the Atlantic coast of Morocco. Micropaleontology 48(3), 257–272.

Weijermars, R., Roep, T.B., Van den Eeckhout, B., Postma, G., Kleverlaan, K., 1985. Uplift history of a Betic fold nappe inferred from Neogene–Quaternary sedimentation and tectonics (in the Sierra Alhamilla and Almería, Sorbas and Tabernas Basins of the Betic Cordilleras, SE Spain). Geol. Mijnb. 64, 397–411.

Young, J.R. (1998) Chapter 9: Neogene. In: Bown, P.R. (Ed.), Calcareous Nannofossils Biostratigraphy, British Micropaleontological Society Publications Series, Kluwer Academic Press, Dordrecht, p. 225–265.

FIGURE CAPTIONS

Fig. 1. Location of the Andalucian Sorbas Basins in the Western Mediterranean and simplified geological map of the studied region.

Grey box delimits the geological maps shown in Figure 3.

Fig. 2. Usual chronostratigraphic scheme of the Sorbas Basin, modified from Martín & Braga (1994), Riding et al. (1998, 1999) and Fortuin et al. (2000), with the proposed locations of the MES: MES 1 (Gautier et al., 1994), MES 2 (Roveri et al., 2009), MES 3 (Riding et al., 1999; Bourillot et al., 2010a). Chronology is from Fortuin et al. (2000).

Fig. 3. Geological map of the Sorbas Basin, modified from Ott d'Estevou (1990).

Main lithologies:

a, Betics basement; b, Volcanic rock;

Tortonian: c, clays and turbidites; d, Algal Limestone (Azagador Member);

Messinian: e, Reef Unit; f, Clays and diatomites (Abad Member); g, Coastal limestone and sandstone; h, Gypsum (Yesares Member);

Zanclean: i, Clays and laminated clays (Sorbas Member); j, Sorbas Limestone (Sorbas Member); k, Red sands and loams (Zorreras Member); l, Marls and calcarenites (Zorreras M.); m, Fluvial conglomerates (Zorreras M.);

Quaternary: n, Caliches, loams, alluvial deposits.

Most important studied localities:

1, Cuesta de Cariatiz; 2, Manantial de los Charcones; 3, Moras; 4, Peñon Díaz quarry; 5, Cortijo del Hoyo; 6, Corral de Juan Cipriano; 7, Panoramic Viewpoint; 8, Cortijo de Paco el Americano; 9, Hostal Sorbas section; 10, Cortijo Marchalien La Gorda section; 11, Zorreras; 12, La Cumbre; 13, Cerro de Juan Contrera; 14, Barranco del Infierno; 15, Torcales del Pocico; 16, Los Molinos de Río Aguas; 17, Cruz del Rojo quarry; 18, Cuevas de Sorbas.

The cross sections shown in Figure 17 are drawn.

Places where the MES has been identified are indicated as the extrapolated course of the Messinian valleys and development of Gilbert-type fan deltas.

Fig. 4. Comparison between various concepts of the Terminal Carbonate Complex (TCC) and its chronostratigraphic location. This comparison is done for the Sorbas Basin between its edges (i.e. reefal) and centre with reference to the concerned stratigraphic units. The variable (chrono) stratigraphic position of the Messinian Erosional Surface is also indicated.

Fig. 5. Chronostratigraphy, including planktonic foraminifers and calcareous nannoplankton biostratigraphies, of the Late Miocene and Pliocene. Chronology refers to Lourens et al. (2005).

The grey strips correspond to two steps of the MSC (Clauzon et al., 1996) accepted by a representative community working on the MSC (CIESM, 2008). Chronology of the end of the MSC is from Bache et al. (2012).

Fig. 6. Simplified location map of the Sorbas area from SGE 1997 (sheet 24-42 – 25-42) (altitude: thick contour lines at 300, 400, 500 and 600 m; thin contour lines at: 340, 360, 440, 460, 540, 560 and 640 m; gypsum quarries are outlined in orange).

Localities: 1, Cuesta de Cariatiz section; 2, Manantial de los Charcones section; 3, Moras section; 4, Gypsum quarry at Peñon Díaz; 5, Cortijo del Hoyo; 6, Corral de Juan Cipriano; 7, Panoramic Viewpoint section; 8, Cortijo de Paco el Americano section (left bank of the Río Aguas) and nannofossil locality (right bank of the Río Aguas); 9, Hostal Sorbas section; 10, Cortijo Marchalien La Gorda section; 11, Zorreras; 12, La Cumbre; 13, Cerro de Juan Contrera; 14, Barranco del Infierno; 15, Torcales del Pocico; 16, Los Molinos de Río Aguas section; 17, Cruz del Rojo quarry; 18, Cuevas de Sorbas.

The cross sections shown in Figure 19 are drawn.

Fig. 7. The Cuesta de Cariatiz section.

A, Section with location of the studied samples.

W1, Lower white chalky layer of the Zorreras Member.

B, View of the Sorbas Basin from the Cariatiz coral reef.

C, Erosional contact of the foreset beds of the Gilbert-type fan delta with the carbonated laminites.

D, Another view of the erosional contact of foreset beds of the Gilbert-type fan delta within alterated carbonated laminites.

E, The Gilbert-type fan delta with location of the studied samples.

W1, lower white chalky layer of the Zorreras Member.

F, Detail of the foreset beds of the Gilbert-type fan delta.

Fig. 8. The Góchar – Moras area.

A, Perspective drawing of the Manantial de los Charcones section (Góchar) at the root of the Gilbert-type fan delta nested within the Reef Unit, with location of the studied sample. Legend, see Figure 7.

B, View of the Manantial de los Charcones section showing the root of the Gilbert-type fan delta nested within the Reef Unit, with location of the studied sample. The dotted red line delimits the Gilbert-type fan delta.

C, Reef carbonate with eroded surface of *Porites* colonies, then bored by saxicavous bivalves.

D, The Moras section with location of the studied sample. Legend, see Figure 7.

E, View of the Moras section where the marine-continental transition has been drawn (dotted black line), with location of the studied sample.

F, Zoom on the marine-continental transition in the Moras section.

G, View of the almost flat abandonment surface of the Góchar – Moras Gilbert-type fan delta (at ca. 455 m in altitude). The top of the Zorreras section can be considered as a residual expression of this surface in the central part of the Sorbas Basin.

Fig. 9. The Cortijo del Hoyo area.

A, View of the Cortijo del Hoyo section with location of the studied samples and place of the view shown in Figure C.

B, Interpreted Cortijo del Hoyo section with location of the analysed samples.

C, View back the hill of the Cortijo del Hoyo section.

D, View of the studied section at Corral de Juan Cipriano with location of the analysed samples, overlain by the Zorreras Member showing its lower white chalky layer (W1).

Fig. 10. The Panoramic Viewpoint area.

A, View of the studied section with location of the analysed samples. The dotted red line indicates the erosional contact.

B, Interpreted section with location of the analysed samples.

Fig. 11. The Cortijo de Paco el Americano area.

A, View of the section located in Figure 7 where the lateral shift between basinal clays and the Sorbas Limestone can be observed.

B, Lithological interpretation of the section with stratigraphic position of samples 1-3 of locality 8 of Figures 3 and 6.

C, Samples taken at locality 8 of Figures 3 and 6.

D, The section in front of Hostal Sorbas with location of the analysed samples (m-c tr., marine-continental transition).

Fig. 12. The Zorreras area at Cortijo Marchalien la Gorda.

A, View from the *Aphanius crassicaudus* beds (Sorbas Member) to the top of the Zorreras Member.

W1, lower white chalky layer of the Zorreras Member.

B, Detail of the *Aphanius crassicaudus* beds and location of the studied samples (1 to 7).

C, Overlying sediments (with location of the studied samples: 8 to 10) including the lower chalky white layer of the Zorreras Member (W1).

Fig. 13. The Zorreras Member.

A, View of the Zorreras section overlying the Sorbas Limestone and showing the stratigraphic location of the three white chalky layers (W1-2-3) and coquina.

B, Lithological sketch of the Zorreras section.

W1-2-3, white chalky layers.

C, View of the middle white chalky layer (W2) in the Zorreras section.

D, View of the upper white chalky layer (W3) and coquina (C) in the Zorreras section.

E, One specimen of the gastropod *Epitonium depressicosta* associated with fragments of echinoids within the basal silts of the Zorreras section.

F, Base of the bivalve coquina mostly composed of *Ostrea lamellosa*.

G, Top of the bivalve coquina with prevalent veneroids.

Fig. 14. The southern part of the Sorbas Basin.

A, Stratigraphy of the La Cumbre – Cerro de Juan Contrera area.

B, Three dimensional Google Earth view of the La Cumbre – Cerro de Juan Contrera area with location of the studied samples.

C, View of the La Cumbre section.

D, Location of the studied samples at La Cumbre: C, coquina.

E, Sample 2 from Cerro de Juan Contrera.

Fig. 15. Messinian erosion of the Yesares Member.

A, Panoramic view of the Messinian and Zanclean series at Los Molinos de Río Aguas.

B, Panoramic oblique view of the Los Molinos de Rio Aguas area showing the spatial relationships between the Abad Member, the gypsums and post-MSC latest Messinian-early Zanclean Sorbas marine sediments accompanied by a debris flow located along the road AL-140. Post-MSC marine deposits are separated from the gypsum beds by an erosional surface there underlined in red. The panoramic view has been realized by wrapping the geological map of the Sorbas Basin on a digital elevation grid (resolution: 10 m) of the basin. Vertical exaggeration: 1.5.

C, Zoom on the Messinian valley of the Río Aguas.

D, Block of reworked gypsum wrapped within debris flow deposit. About 600 m to the east of the pass, blocks of gypsum have been rightly considered as fallen off the gypsum cliff onto the underlying Abad diatomites-clays, i.e. being a slope deposit (Braga et al., 2006). Major differences between these categories of gypsum blocks can be outlined: (1) the blocks of gypsum wrapped within an heterogeneous matrix, that we refer to a debris flow, are only located at the pass of Los Molinos de Río Aguas, (2) eslsewhere, there are isolated blocks of gypsum resulting from recent breaking up which are not included in a matrix but rather resting on the Abad marls (see A and B).

E, Detail of the debris flow composed of various reworked elements (yellow marls, grey clays, schists, etc.).

Fig. 16. Cross sections through the Sorbas Basin resulting from our field observations and interpretation (location in Figures 3 and 7).

A, From Cuesta de Cariatiz to Río Aguas; B, From Zorreras to Los Molinos de Río Aguas.

Fig. 17. Usual chronostratigraphic scheme of the Sorbas Basin modified according to our field observations, biostratigraphic data and interpretation.

Fig. 18. Chronological frame of the sedimentary series which deposited in the Sorbas Basin between 6.2 and 5.0 Ma with respect to the tectonic evolution of the Gibraltar region and compared to those of the Mediterranean central basins.

Chronology refers to bioevents [planktonic foraminifers from Lourens et al. (2005), calcareous nannofossils from Raffi et al. (2006)], to astrochronology of the Sorbas gypsums (Manzi et al., 2013), to oxygen isotope reference curve from ODP Site 982 (Hodell et al., 2001: Northeastern Atlantic) and global sea level changes (Miller et al., 2011).

The curve of percentage of the neritic dinoflagellate cyst *Operculodinium israelianum* from the Salé briqueterie (Bou Regreg, Morocco) (Warny et al., 2003) is correlated with the $\delta^{18}O$ record at Site 982 by Hodell et al. (2001).

Fig. 19. Process of "aggradation epigenesis" (Clauzon, 1996) applied to the Río Aguas.

A, Cutting of the subaerial Messinian valley of Río Aguas at 5.600 Ma.

B, Zanclean ria after marine reflooding of the Mediterranean at 5.460 Ma marked by deposition of debris flow including blocks of reworked gypsum.

C, Sedimentary filling of the Zanclean ria and aggradation of the alluvial fan of Río Aguas shifted to East at about 4.500 Ma.

D, Quaternary cutting of the modern valley of Río Aguas starting at the onset of glacial in the Northern Hemisphere (2.588 Ma) and uplift of edges of the Sorbas Basin.

E, Present-day state.

Table 1. Longitude – latitude of localities shown in Figures 3 and 6.

Table 2a, b & c. Results from the nannofossil analyses in the Sorbas Basin.

Table 3. Results from the foraminifer analysis at Cerro de Juan Contrera.

Plate 1. Nannofossils from the Sorbas Basin.

Fig. 1, *Ceratolithus acutus* Gartner & Bukry (crossed nicols) from Cortijo del Hoyo (sample 5).

Fig. 2, *Ceratolithus acutus* Gartner & Bukry (crossed nicols) from La Cumbre (sample 6).

Fig. 3, *Ceratolithus acutus* Gartner & Bukry (crossed nicols) from La Cumbre (sample 5).

Fig. 4, *Amaurolithus primus* (Bukry & Percival) Gartner & Bukry (parallel light) from Barranco del Infierno (sample 3).

Figs. 5, and 6, *Discoaster quinqueramus* Gartner (parallel light) from Cortijo del Hoyo (sample 1).

Fig. 7, *Triquetrorhabdulus rugosus* Bramlette & Wilcoxon (parallel light) from La Cumbre, sample 1.

Plate 2. Scanning Electron Microscope pictures of stratigraphically significant planktonic foraminifers from Cerro de Juan Contrera (sample 6).

Fig. 1, *Hirsutella* (*Globorotalia*) *margaritae* (Bolli & Bermudez) in umbilical (a), edge (b) and spiral (c) views.

Fig. 2, *Globoturborotalita nepenthes* Todd in umbilical (a) and edge (b) views.

Scale bars represent 100 μm for all pictures.

N°	Locality	North Latitude	West Longitude
1	Cuesta de Cariatiz	37°8’ 30.20”	2°5’ 5.50”
2	Manantial de los Charcones	37°8’ 10.40”	2°8’ 59.96”
3	Moras	37°8’ 10.40”	2°8’ 29.70”
4	Peñon Díaz quarry	37°5’ 3.10”	2°5’ 20.10”
5	Cortijo del Hoyo	37°6’ 24.50”	2°4’ 46.90”
6	Corral de Juan Cipriano	37°6’ 43.10”	2°4’ 49.90”
7	Panoramic Viewpoint	37°5’ 38.80”	2°5’ 12.00”
8	Cortijo de Paco el Americano	37°5’ 41.00”	2°7’ 26.60”
9	Hostal Sorbas	37°5’ 49.50”	2°7’ 39.60”
10	Cortijo Marchalien La Gorda	37°6’ 11.00”	2°6’ 36.20”
11	Zorreras	37°6’ 9.30”	2°6’ 46.20”
12	La Cumbre	37°4’ 31.00”	2°7’ 58.50”
13	Cerro de Juan Contrera	37°4’ 39.00”	2°7’ 47.00”
14	Barranco del Infierno	37°4’ 45.70”	2°7’ 29.70”
15	Torcales del Pocico	37°4’ 52.70”	2°7’ 24.20”
16	Los Molinos de Río Aguas	37°5’ 24.53”	2°4’ 47.05”
17	Cruz del Rojo quarry	37°7’148.84”	2°4’ 37.9”8
18	Cuevas de Sorbas	37°5’ 29.21”	2°6’ 25.23”

Samples	*Amaurolithus delicatus*	*Amaurolithus primus*	*Braarudosphaera bigelowii*	*Calcidiscus leptoporus*	*Calcidiscus macintyrei*	*Ceratolithus acutus*	*Coccolithus pelagicus*	*Cryptococcolithus mediaperforatus*	*Discoaster asymmetricus*	*Discoaster brouweri* group	*Discoaster quinqueramus*	*Discoaster variabilis*	*Helicosphaera intermedia*	*Helicosphaera kamptneri*	*Helicosphaera orientalis*	*Helicosphaera sellii*	*Helicosphaera stalis*	*Pontosphaera multipora*	*Pontosphaera japonica*	*Reticulofenestra pseudoumbilicus*	*Rhabdosphaera clavigera*	*Scyphosphaera* spp.	Small reticulofenestrids	*Sphenolithus abies*	*Syracosphaera pulchra*	*Thoracosphaera* spp.	*Triquetrorhabdulus rugosus*	*Umbilicosphaera sibogae*
2		x	x	x		x	x													x		x					x	
1		x	x	x		x	x													x		x					x	
Cuesta de Cariatiz																												
1	x		x	x		x	x						x	x			x			x			x	x		x	x	
Moras																												
1		x		x	x		x													x			x	x		x	x	x
Manantial de los Charcones																												
5							x													x			x					
4							x													x			x					
3	x						x							x						x			x	x		x	x	
2			x				x													x			x					
1			x				x							x						x			x			x	x	
Peñon Díaz quarry																												
28							x							x						x			x	x				
27			x	x	x	x	x		x					x				x		x			x	x		x		
26			x	x	x	x	x		x					x				x		x			x	x		x		
25							x							x						x			x	x				
9			x	x	x	x	x							x						x			x	x				
8				x		x	x							x				x	x	x		x		x				
7			x	x		x	x							x						x				x	x			
6				x	x	x	x		x					x		x		x		x	x		x	x		x	x	
5	x		x	x		x	x			x				x	x	x				x			x	x		x	x	
4	x		x	x		x	x							x		x				x			x	x		x	x	
1	x		x	x			x	x		x	x	x		x	x	x		x		x		x	x	x		x	x	x
Cortijo del Hoyo																												
6				x			x													x			x					
5				x			x													x			x					
4		x		x			x							x		x				x			x	x			x	
3				x			x													x			x					
2		x		x			x							x		x				x			x	x			x	
1		x		x			x							x		x				x			x	x			x	
Coral de Juan Cipriano																												

a

Samples	*Amaurolithus delicatus*	*Amaurolithus primus*	*Braarudosphaera bigelowii*	*Calcidiscus leptoporus*	*Calcidiscus macintyrei*	*Ceratolithus acutus*	*Coccolithus pelagicus*	*Discoaster brouweri* group	*Discoaster variabilis*	*Helicosphaera kamptneri*	*Helicosphaera orientalis*	*Helicosphaera sellii*	*Pontosphaera multipora*	*Reticulofenestra pseudoumbilicus*	*Rhabdosphaera clavigera*	*Scyphosphaera* spp.	Small reticulofenestrids	*Sphenolithus abies*	*Thoracosphaera* spp.	*Triquetrorhabdulus rugosus*
26			x	x	x	x	x	x		x			x	x			x	x	x	
25							x			x				x			x	x		
24			x	x	x		x	x		x			x	x			x	x	x	x
23			x	x	x		x	x		x			x	x			x	x	x	x
20	x			x		x	x			x		x		x			x	x	x	x
19	x		x	x		x	x			x				x			x	x	x	x
12				x	x	x	x		x	x		x		x	x	x	x	x	x	x
9	x		x	x	x		x			x		x		x			x	x		x
8		x	x	x			x			x		x		x			x	x		x
7				x			x			x		x		x			x	x		x
6		x		x			x			x		x		x			x	x		x
5			x	x	x	x	x	x		x			x	x			x	x	x	
4							x			x				x			x	x		
3			x	x	x		x			x			x	x			x	x	x	x
2			x	x	x		x			x			x	x			x	x	x	x

Panoramic Viewpoint

3		x	x			x								x		x				x
2	x	x	x	x			x			x				x		x	x	x		x

Cortijo de Paco el Americano

8		x	x			x	x			x	x		x	x			x	x	x	
6							x							x			x	x		
5							x							x			x	x		
4							x							x			x	x		
3						x	x			x				x			x	x	x	x
1		x					x			x	x			x			x	x	x	x

Hostal Sorbas

b

Samples	*Amaurolithus delicatus*	*Amaurolithus primus*	*Braarudosphaera bigelowii*	*Calcidiscus leptoporus*	*Calcidiscus macintyrei*	*Ceratolithus acutus*	*Ceratolithus atlanticus*	*Coccolithus pelagicus*	*Discoaster asymmetricus*	*Discoaster pentaradiatus*	*Discoaster* sp.	*Helicosphaera kamptneri*	*Helicosphaera sellii*	*Pontosphaera multipora*	*Pontosphaera japonica*	*Reticulofenestra pseudoumbilicus*	*Rhabdosphaera clavigera*	*Scyphosphaera* spp.	Small reticulofenestrids	*Sphenolithus abies*	*Thoracosphaera* spp.	*Triquetrorhabdulus rugosus*
10				x		x		x			x	x				x			x	x	x	x
9				x		x		x				x				x			x	x		x
8				x				x				x				x			x	x		
7				x		x		x				x	x			x			x	x	x	x
6			x	x		x		x			x	x	x			x			x	x	x	x
5				x				x				x				x			x	x		
4				x				x				x				x			x	x		
3				x				x				x				x			x	x		
2				x				x				x				x			x	x		
Cortijo Marchalien la Gorda																						
6	x		x	x		x		x				x	x			x			x	x	x	x
5	x			x		x		x				x	x			x			x	x		
1	x		x	x				x				x	x			x			x	x	x	x
La Cumbre																						
6				x	x			x				x		x	x	x	x		x	x		
5			x	x				x				x		x		x	x		x	x		
4		x		x	x		x	x				x		x		x	x		x	x		x
3			x	x				x				x		x		x	x		x			x
2	x	x	x	x		x		x	x	x		x		x		x	x		x	x		x
Cerro de Juan Contrera																						
3	x	x	x	x		x										x		x		x	x	x
2	x	x	x			x										x		x				
1		x	x			x		x								x						
Barranco del Infierno																						
3			x	x		x		x				x				x			x		x	x
Torcales del Pocico																						

c

Samples	*Dentoglobigerina altispira*	*Globigerina bulloides*	*Globigerina falconensis*	*Globigerinella siphonifera*	*Globigerinita glutinata*	*Globigerinita uvula*	*Globigerinoides conglobatus*	*Globigerinoides extremus*	*Globigerinoides obliquus*	*Globigerinoides quadrilobatus*	*Globigerinoides ruber*	*Globigerinoides sacculifer*	*Globigerinoides trilobus*	*Globorotalia plesiotumida*	*Hirsutella* (*Globorotalia*) *margaritae*	*Globorotalia scitula*	*Globorotalia tumida*	*Globoturborotalita decoraperta*	*Globoturborotalita nepenthes*	*Neogloboquadrina acostaensis*	*Neogloboquadrina humerosa*	*Orbulina bilobata*	*Orbulina universa*	*Sphaeroidinellopsis seminulina*	*Turborotalia humilis*	*Turborotalia quinqueloba*
6		x	x	x		x	x	x	x	x		x	x	x	x	x		x	x	x	x	x	x			x
4	x	x		x	x	x		x	x	x		x	x	x	x	x	x	x		x			x			x
3		x	x	x				x	x	x		x	x	x				x	x				x			
2		x		x			x	x	x	x		x	x	x		x	x	x	x	x	x		x		x	
1		x		x				x	x	x	x	x	x	x		x	x	x	x	x	x		x	x		

Cerro de Juan Contrera

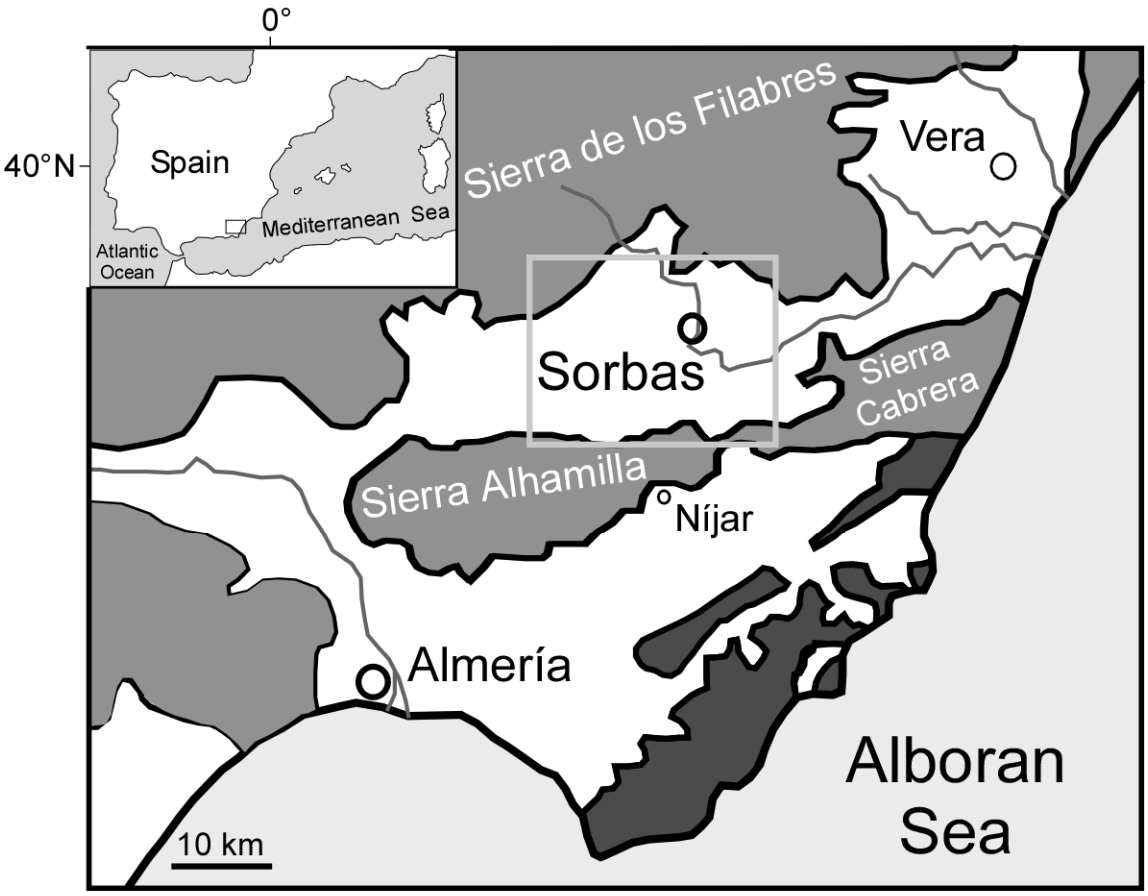
0°
40°N
Spain
Mediterranean Sea
Atlantic Ocean
Sierra de los Filabres
Vera
Sorbas
Sierra Cabrera
Sierra Alhamilla
Níjar
Almería
Alboran Sea
10 km
Neogene and Quaternary sediments
Neogene volcanic rocks
Metamorphic rocks of the Betic Ranges

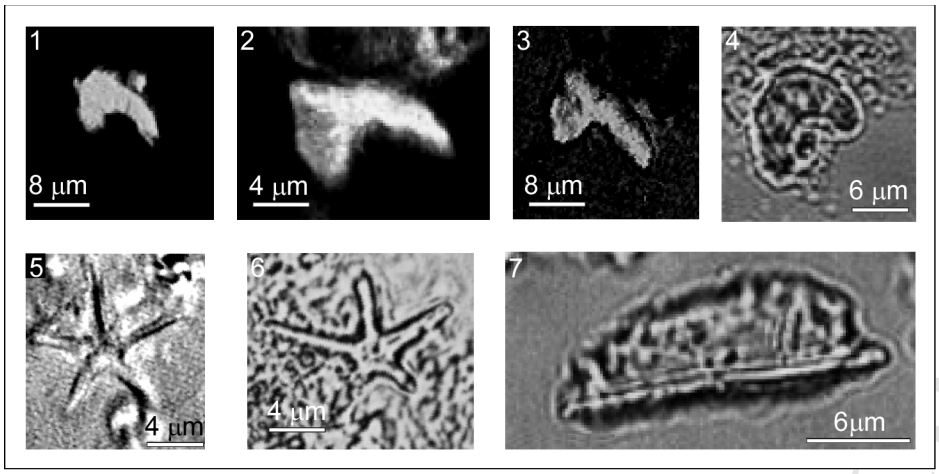

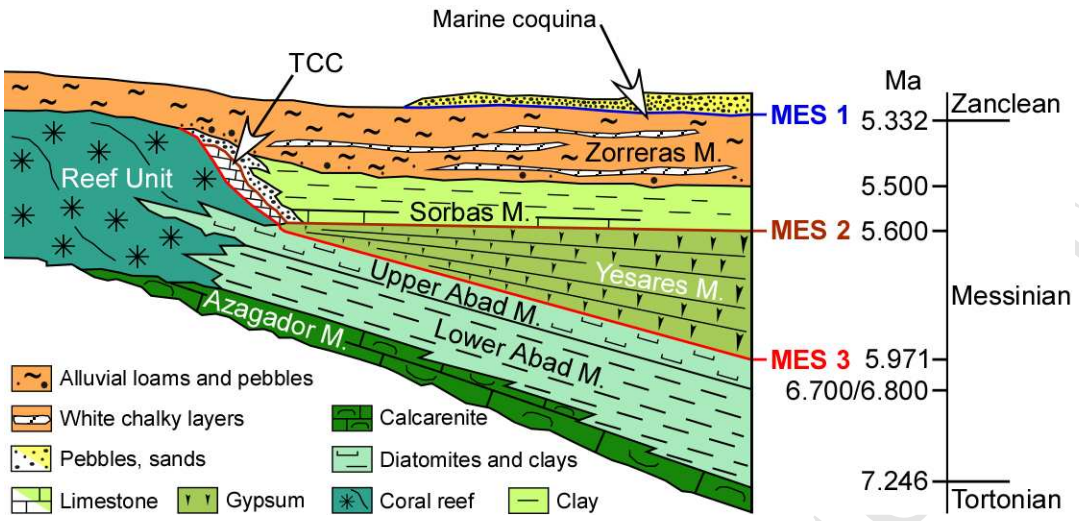

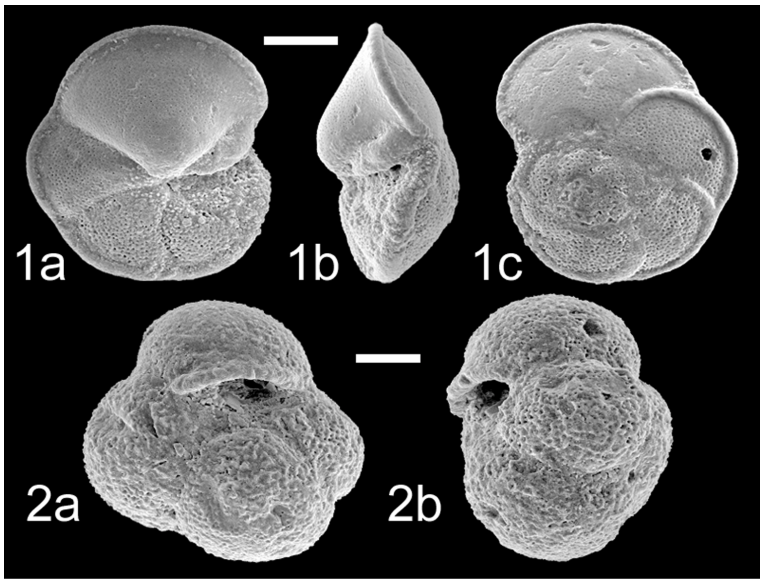

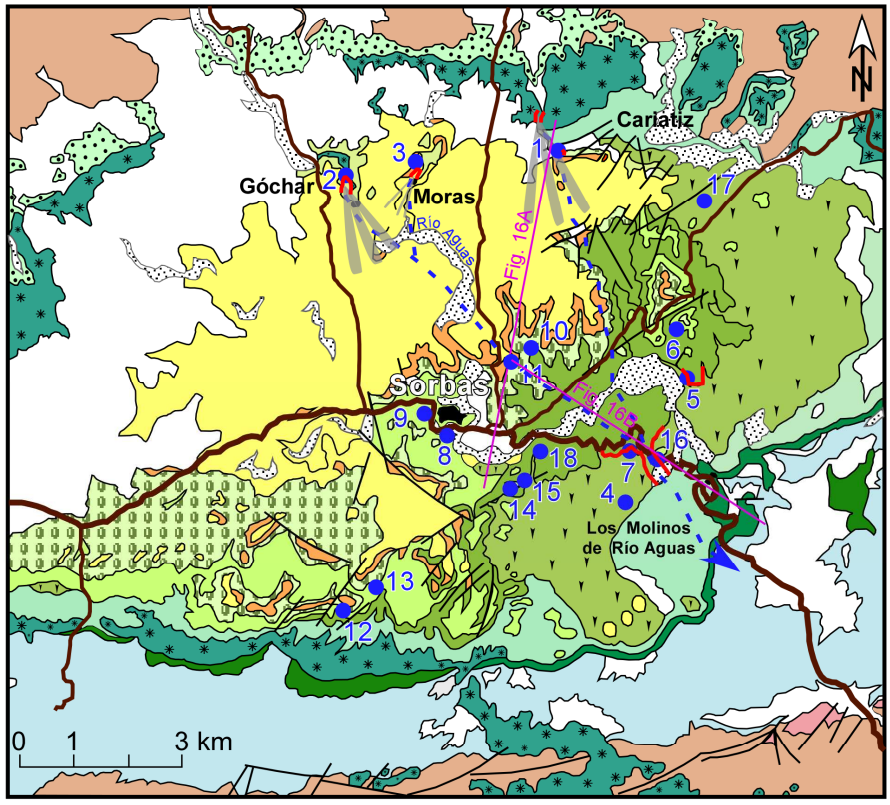
N
Cariatiz
Góchar
Moras
Río Aguas
Fig. 16A
Fig. 16B
Sorbas
Los Molinos de Río Aguas
1
2
3
4
5
6
7
8
9
10
11
12
13
14
15
16
17
18
0 1 3 km
a b c d e f g h i j k l m n
Observed erosional surface
Extrapolated course of the valleys
Development of the prograding sediments of the Gilbert-type fan deltas

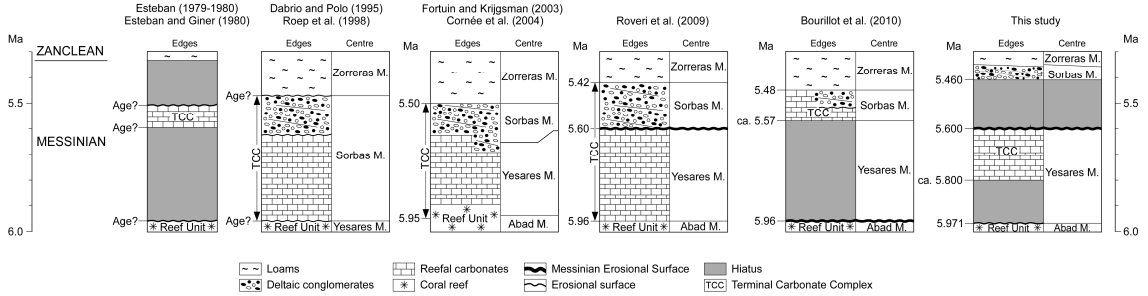

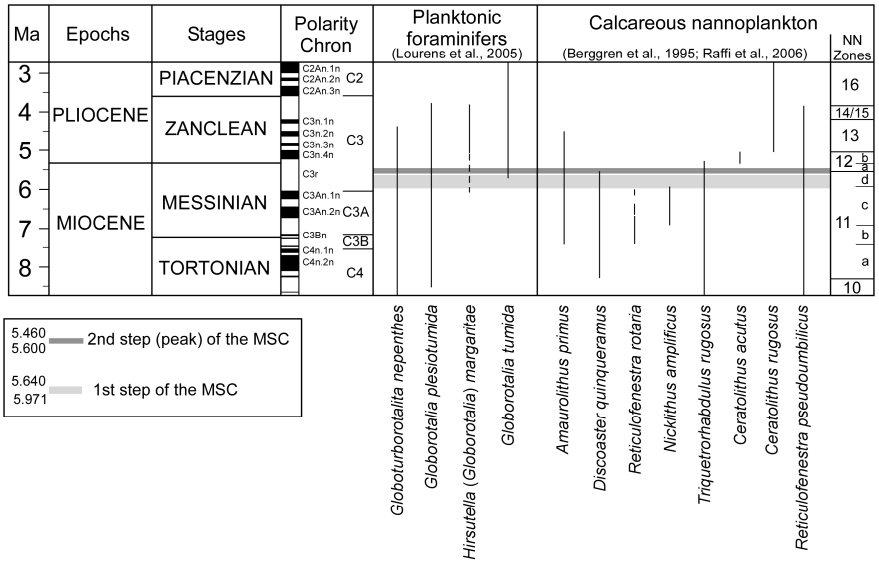

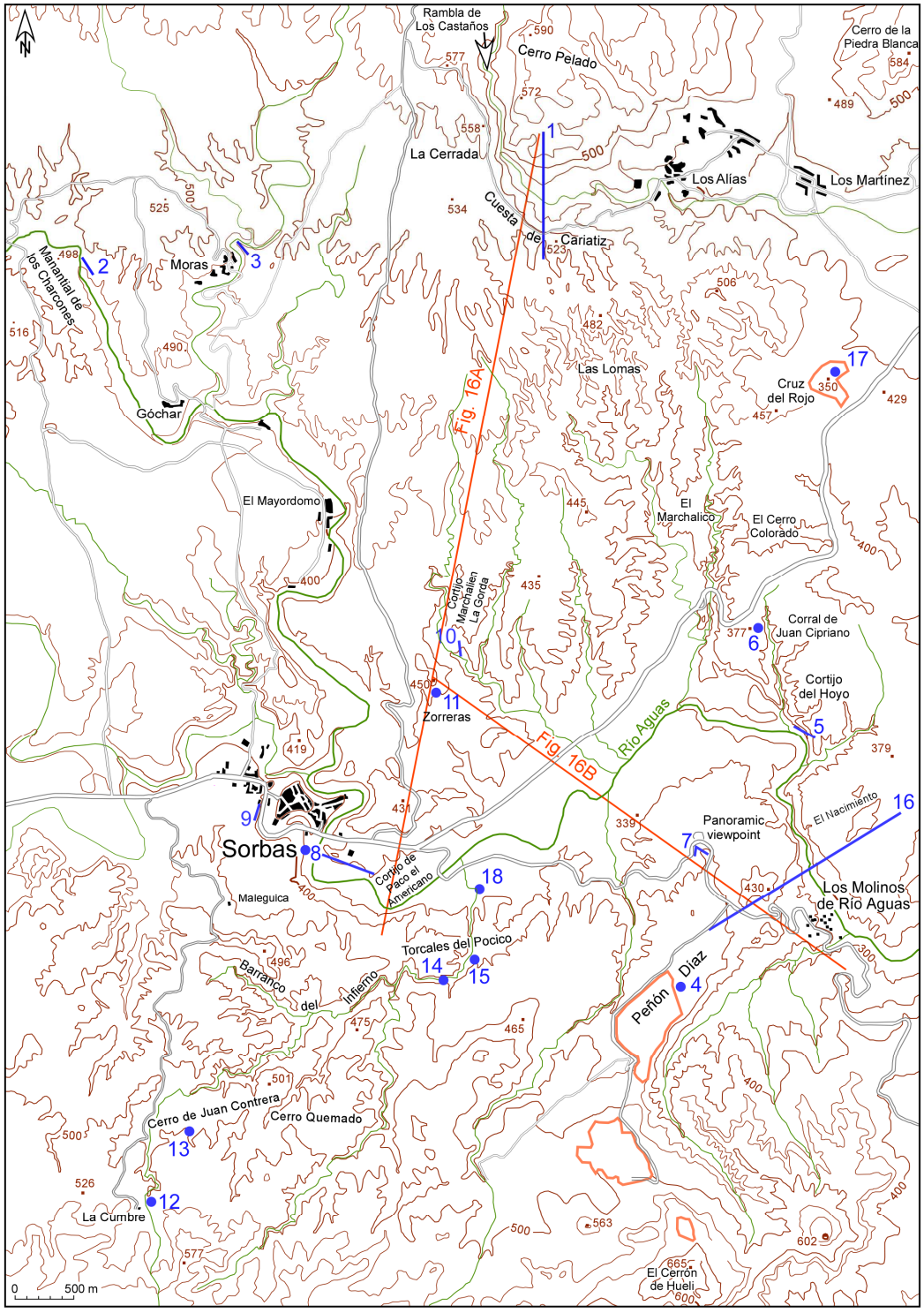
Rambla de Los Castaños
Cerro Pelado
Cerro de la Piedra Blanca
La Cerrada
Los Alías
Los Martínez
Cuesta de Cariatiz
Manantial de los Charcones
Moras
Góchar
Las Lomas
Cruz del Rojo
Fig. 16A
El Mayordomo
El Marchalico
El Cerro Colorado
Corral de Juan Cipriano
Cortijo Marchalen La Gorda
Cortijo del Hoyo
Zorreras
Río Aguas
Fig. 16B
El Nacimiento
Panoramic viewpoint
Sorbas
Cortijo de Paco el Americano
Maleguica
Los Molinos de Río Aguas
Torcales del Pocico
Barranco del Infierno
Díaz
Peñón
Cerro de Juan Contrera
Cerro Quemado
La Cumbre
El Cerrón de Hueli
0
500 m

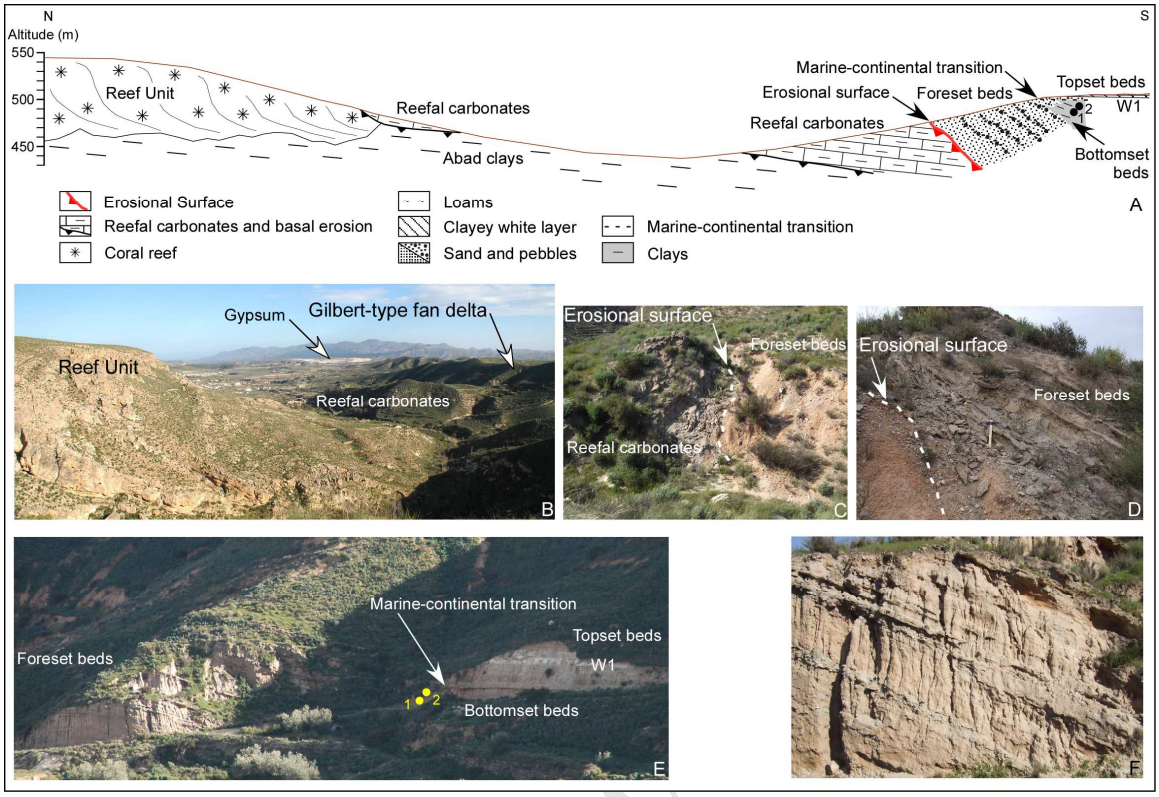

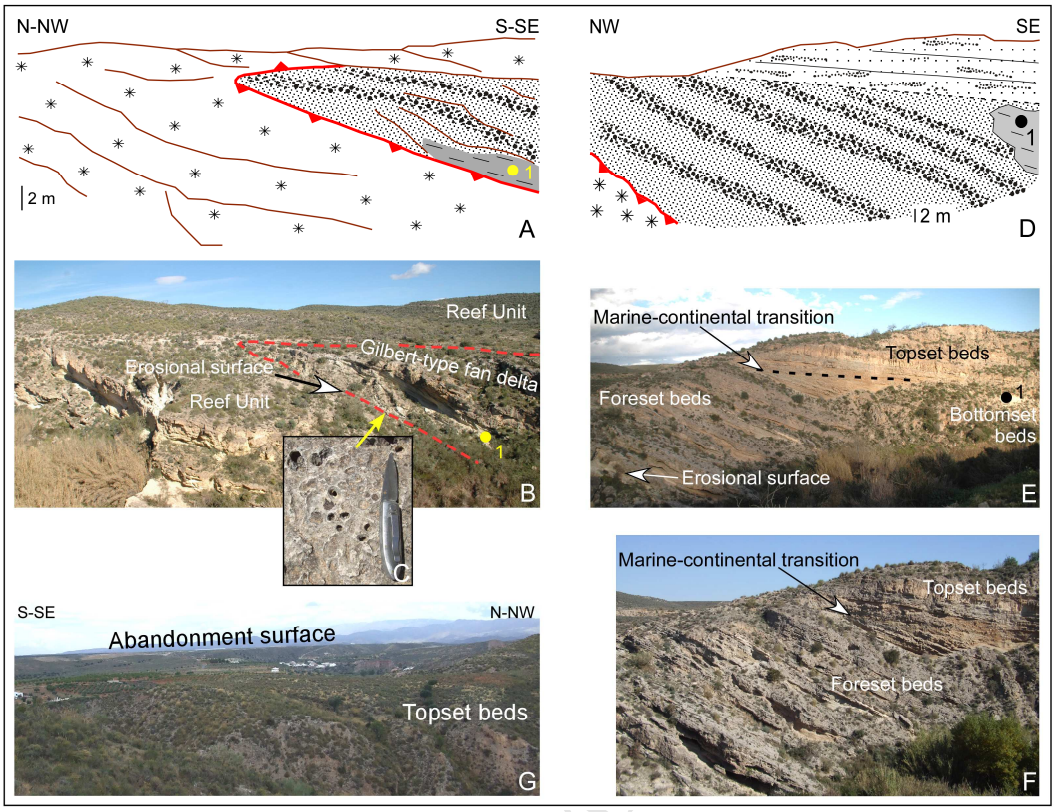

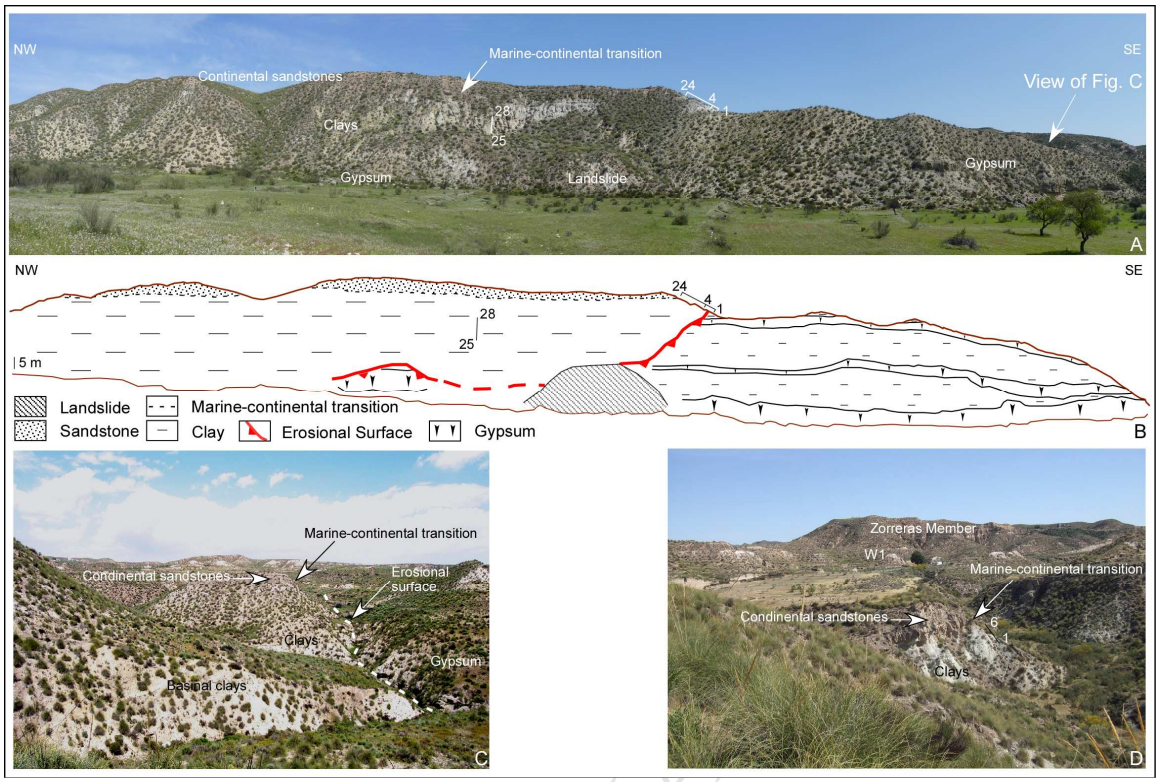

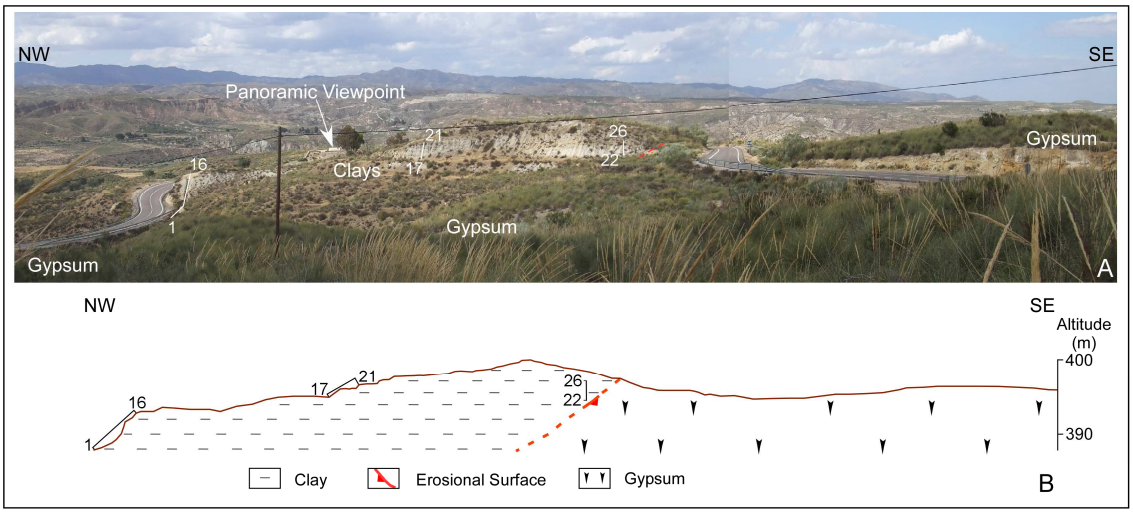

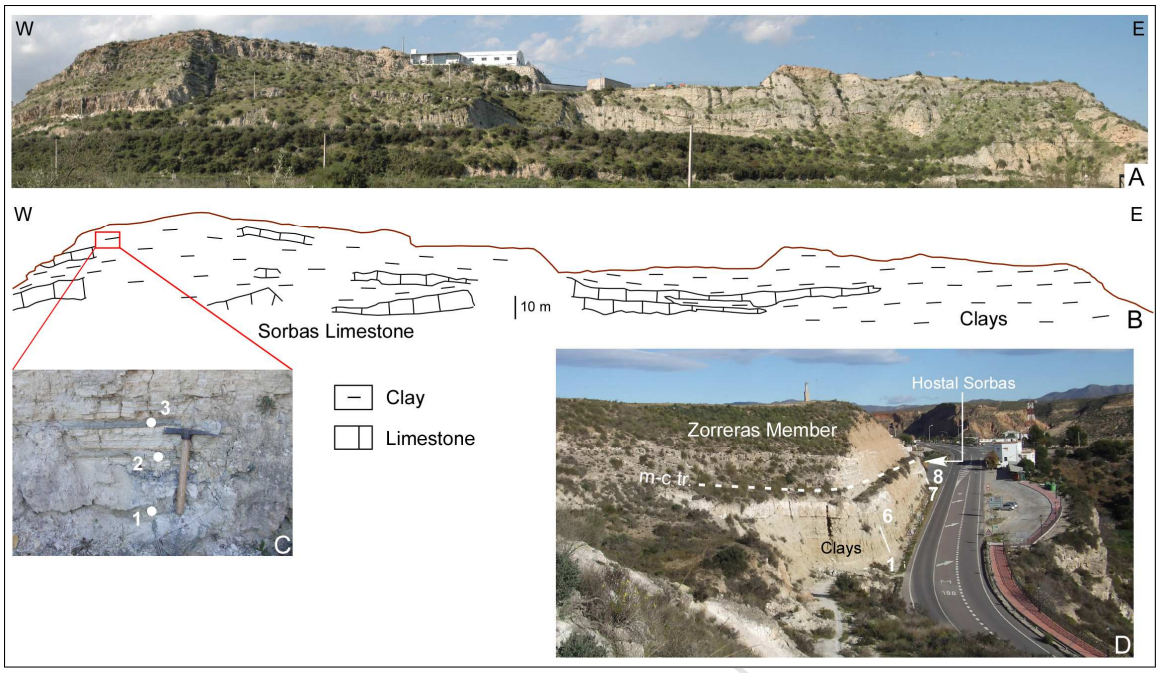

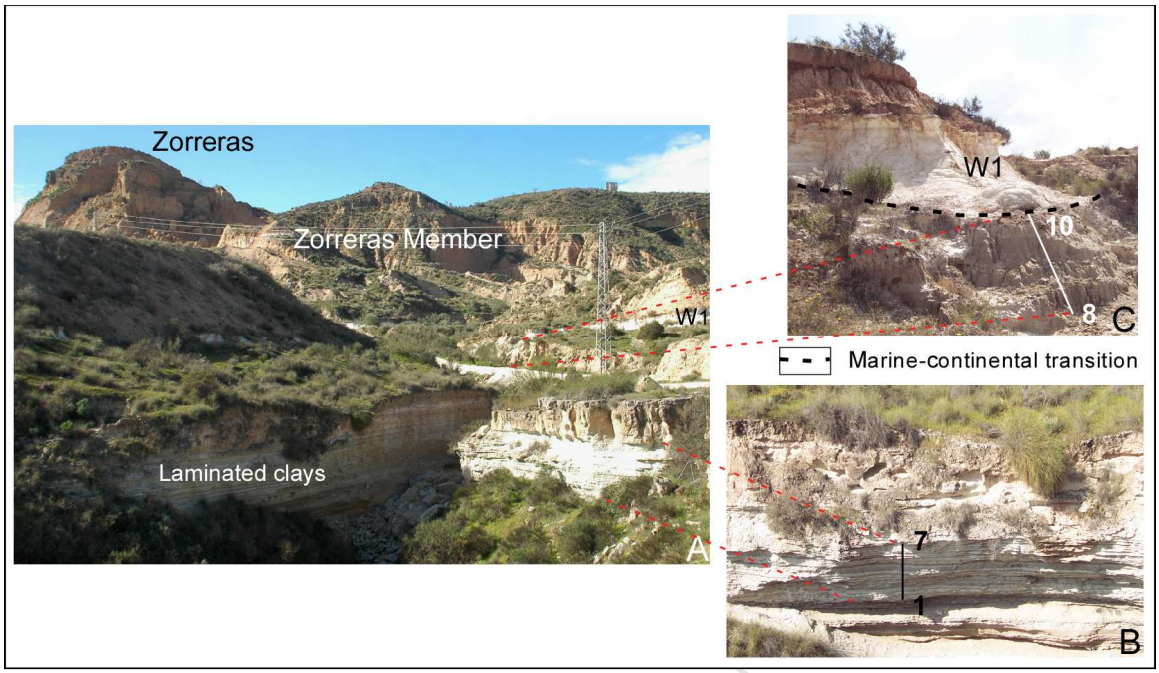

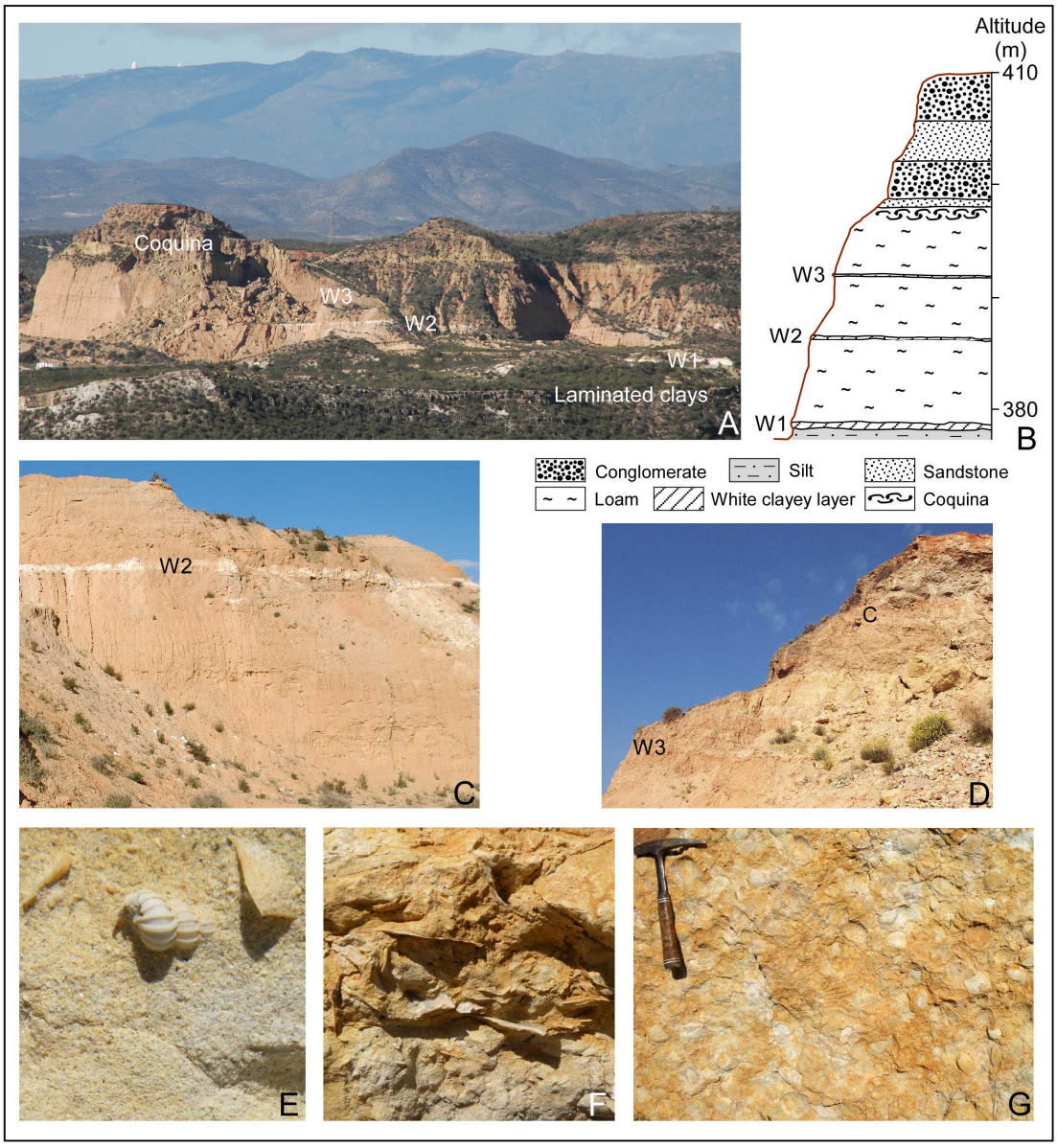
Coquina
W3
W2
W1
Laminated clays
A
Altitude
(m)
410
380
W3
W2
W1
B
Conglomerate
Silt
Sandstone
Loam
White clayey layer
Coquina
W2
C
C
W3
D
E
F
G

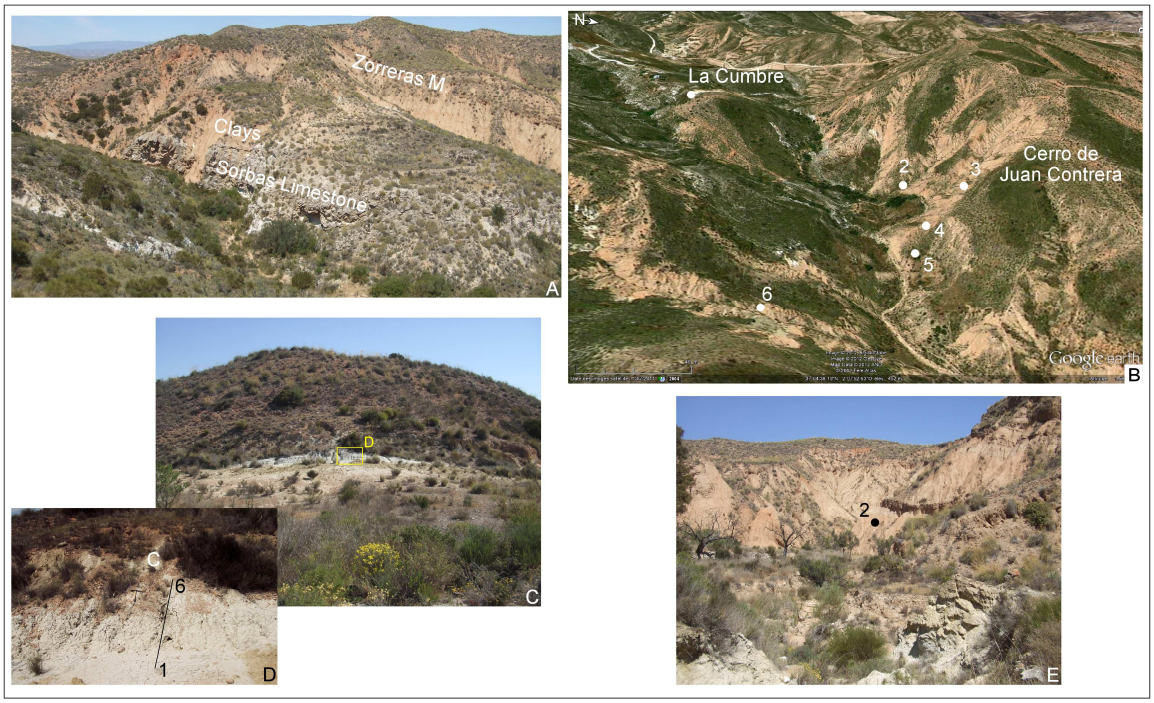
Zorreras M
Clays
Sorbas Limestone
A
N
La Cumbre
2
3
Cerro de
Juan Contrera
4
5
6
Google earth
B
D
C
C
6
1
D
2
E

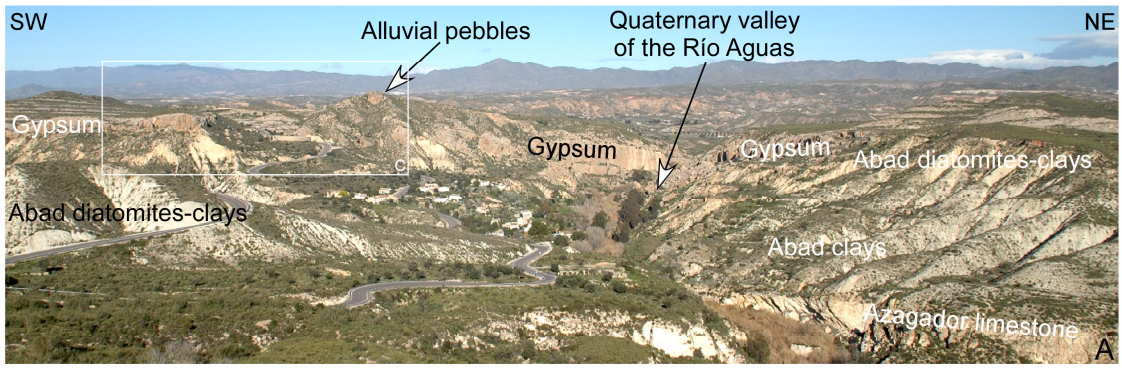
SW
Alluvial pebbles
Quaternary valley
of the Río Aguas
NE
Gypsum
Gypsum
Gypsum
Abad diatomites-clays
Abad diatomites-clays
Abad clays
Azagador limestone
A

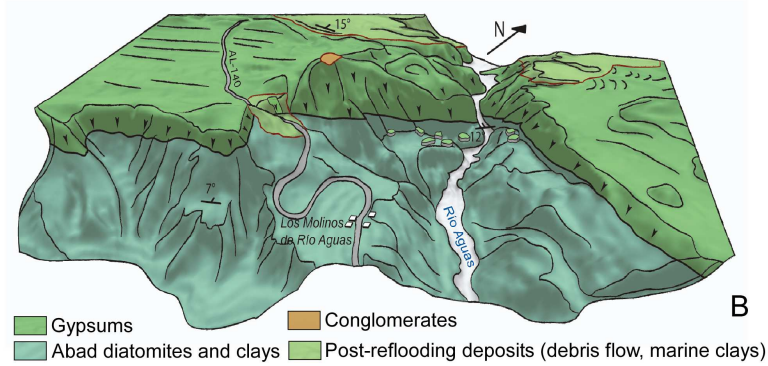
N
15°
7°
AL-140
Los Molinos
de Río Aguas
Río Aguas
B
Gypsums
Conglomerates
Abad diatomites and clays
Post-reflooding deposits (debris flow, marine clays)

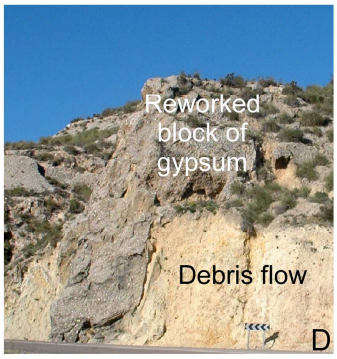
Reworked
block of
gypsum
Debris flow
D

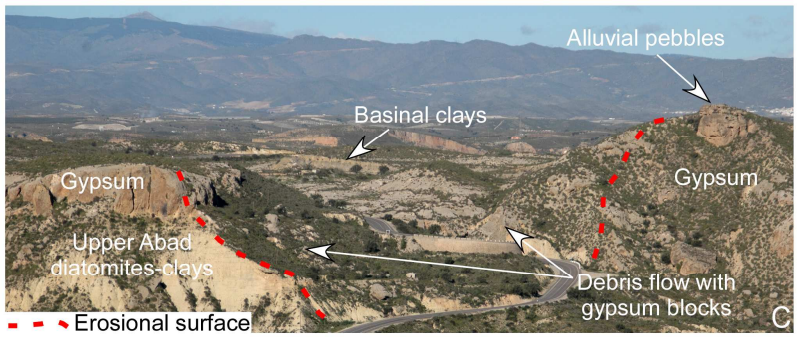
Alluvial pebbles
Basinal clays
Gypsum
Gypsum
Upper Abad
diatomites-clays
Debris flow with
gypsum blocks
Erosional surface
C


E

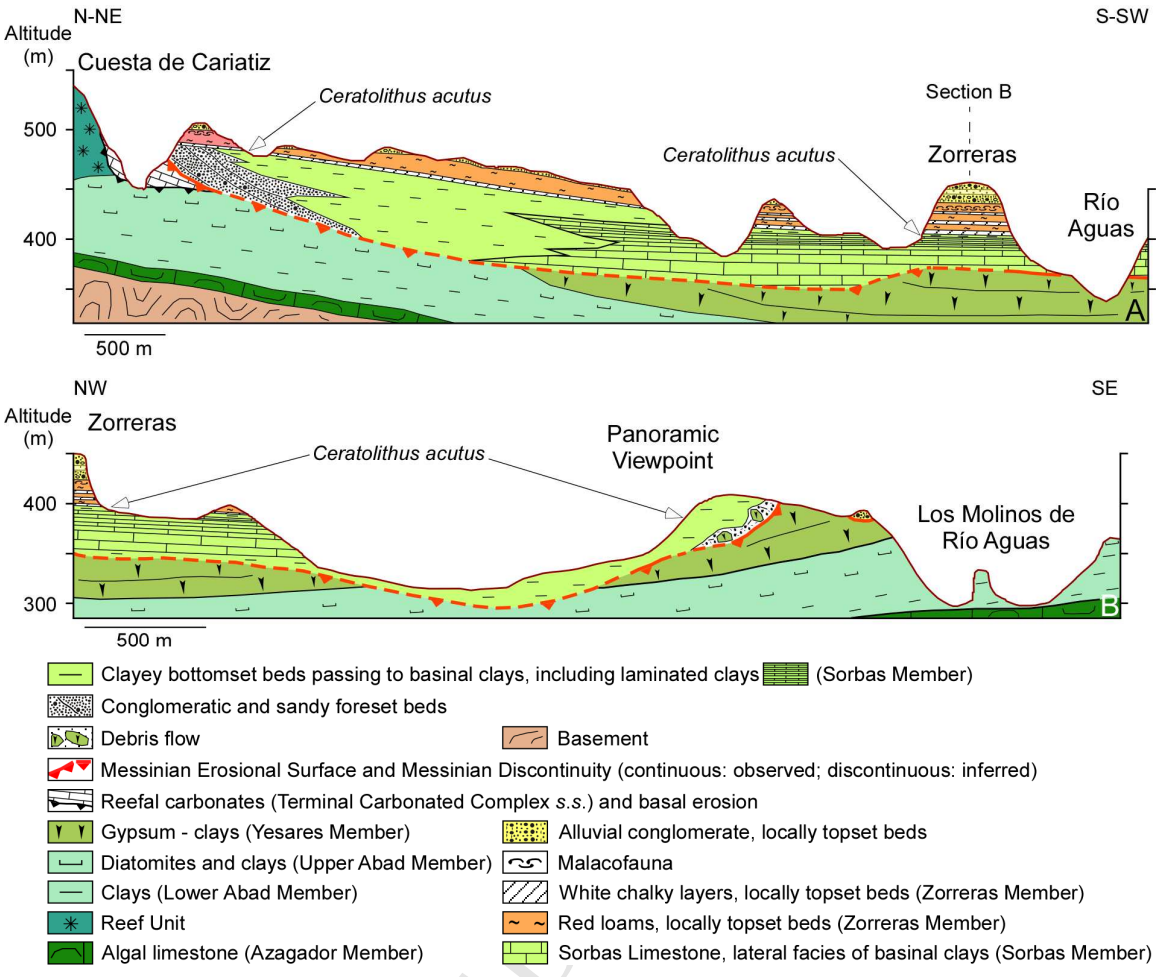

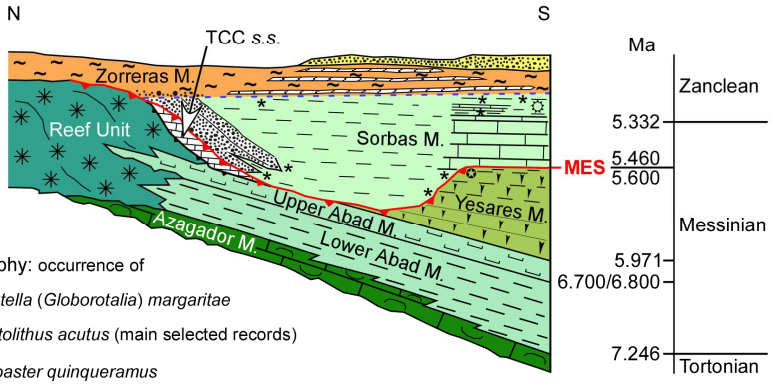

Biostratigraphy: occurrence of

- *Hirsutella* (*Globorotalia*) *margaritae*
- *Ceratolithus acutus* (main selected records)
- *Discoaster quinqueramus*

Zanclean to Quaternary:

- Conglomerates

Latest Messinian - Zanclean Gilbert-type fan deltas (from 5.460 Ma):

- Zorreras Member: white chalky layers (part of topset beds and their basinal correlative)
- Zorreras Member: red loams, alluvial pebbles ans sandstones (part of topset beds and their basinal correlative)
- Marine-continental transition
- Conglomeratic and sandy foreset beds
- Sorbas Member: clayey bottomset beds passing to basinal clays (including laminated clays) and the Sorbas Limestone

Messinian (7.246 - 5.460 Ma):

- Messinian Erosional Surface, Messinian Discontinuity (5.600 - 5.460 Ma)
- Terminal Carbonated Complex: Reefal carbonates (ca. 5.800 - 5.600 Ma) and basal erosion
- Gypsum - clays (Yesares Member: 5.971 - 5.600 Ma)
- Clays, diatomites and clays

Tortonian to Messinian:

- Reef Unit

Tortonian:

- Algal limestone (Azagador Member)

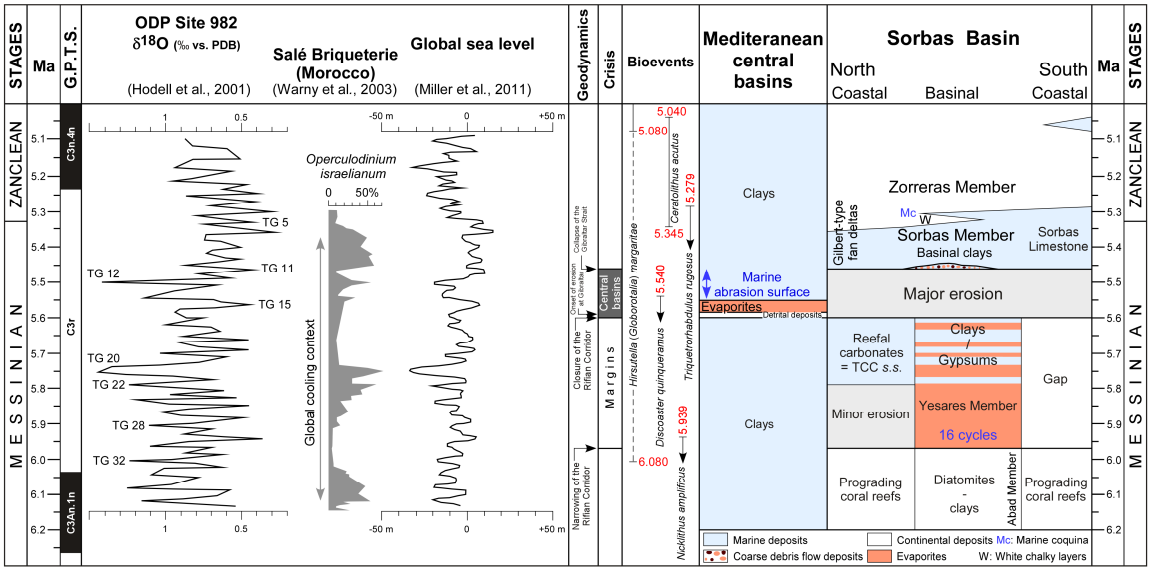

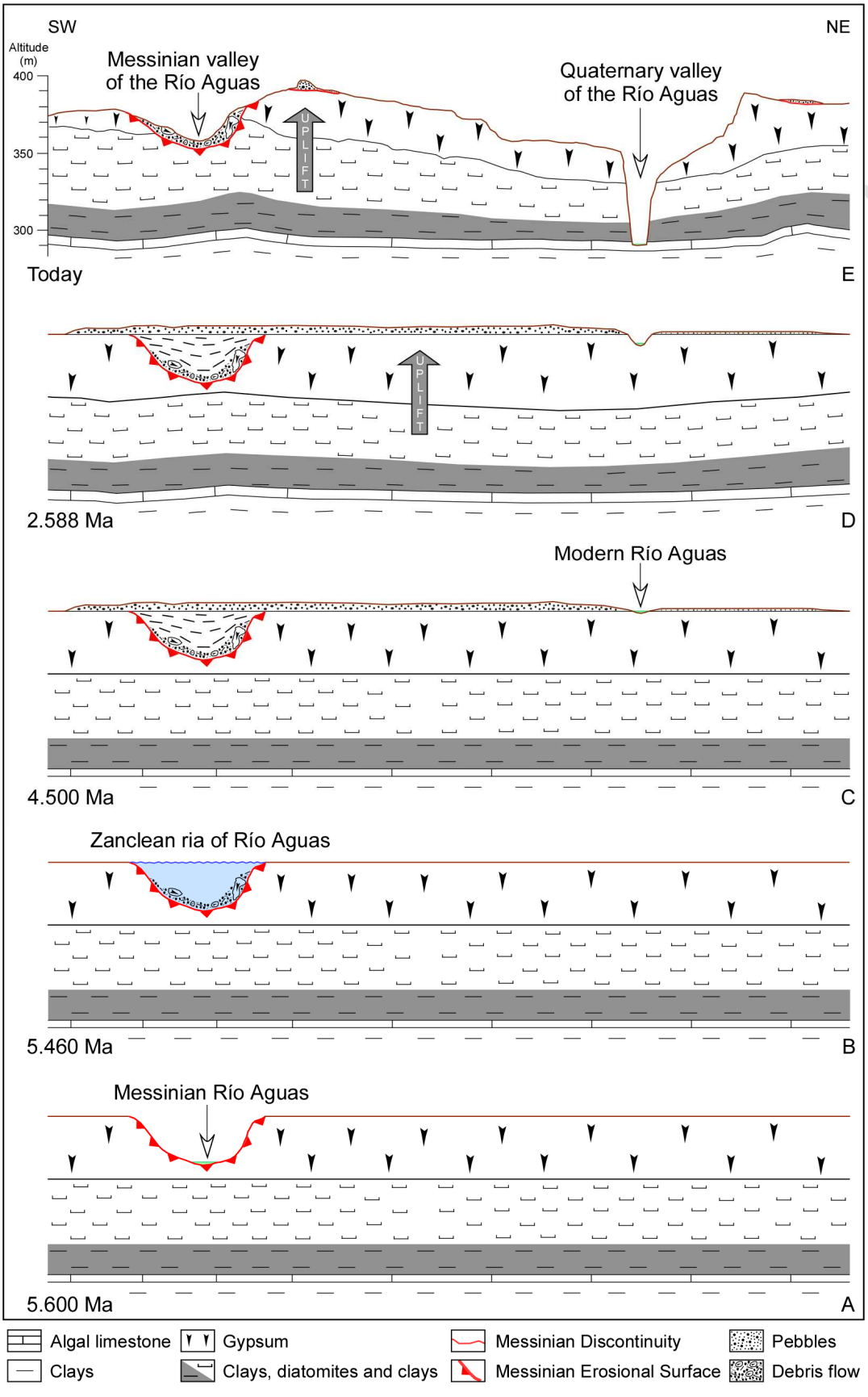
SW
NE
Altitude (m)
400
350
300
Messinian valley of the Río Aguas
Quaternary valley of the Río Aguas
UPLIFT
Today
E
UPLIFT
2.588 Ma
D
Modern Río Aguas
4.500 Ma
C
Zanclean ria of Río Aguas
5.460 Ma
B
Messinian Río Aguas
5.600 Ma
A
Algal limestone
Gypsum
Messinian Discontinuity
Pebbles
Clays
Clays, diatomites and clays
Messinian Erosional Surface
Debris flow

Highlights: >The Sorbas Basin documents the Messinian Salinity Crisis (MSC) two-step scenario. >Subaerial erosion significantly affected the Yesares gypsums during the MSC peak. >The Sorbas Member marks the post-MSC marine reflooding of the Mediterranean Basin. >The Terminal Carbonate Complex must be restricted to carbonated constructions. >The Zorreras Member, which includes the Lago Mare facies, is Zanclean in age.